



HAL
open science

Differential contribution of plant-beneficial functions from *Pseudomonas kilonensis* F113 to root system architecture alterations in *Arabidopsis thaliana* and *Zea mays*

Jordan Vacheron, Guilhem Desbrosses, Sébastien Renoud, Rosa-Maria Padilla-Aguilar, Vincent Walker, Daniel Muller, Claire Prigent-Combaret

► To cite this version:

Jordan Vacheron, Guilhem Desbrosses, Sébastien Renoud, Rosa-Maria Padilla-Aguilar, Vincent Walker, et al.. Differential contribution of plant-beneficial functions from *Pseudomonas kilonensis* F113 to root system architecture alterations in *Arabidopsis thaliana* and *Zea mays*. *Molecular Plant-Microbe Interactions*, 2017, 31 (2), 10.1094/MPMI-07-17-0185-R . hal-01613633

HAL Id: hal-01613633

<https://hal.science/hal-01613633>

Submitted on 27 May 2020

HAL is a multi-disciplinary open access archive for the deposit and dissemination of scientific research documents, whether they are published or not. The documents may come from teaching and research institutions in France or abroad, or from public or private research centers.

L'archive ouverte pluridisciplinaire **HAL**, est destinée au dépôt et à la diffusion de documents scientifiques de niveau recherche, publiés ou non, émanant des établissements d'enseignement et de recherche français ou étrangers, des laboratoires publics ou privés.

1 **Differential contribution of plant-beneficial functions from**
2 ***Pseudomonas kilonensis* F113 to root system architecture**
3 **alterations in *Arabidopsis thaliana* and *Zea mays***

4

5

6

7 Jordan Vacheron^{1#}, Guilhem Desbrosses², Sébastien Renoud¹, Rosa Padilla¹, Vincent
8 Walker¹, Daniel Muller¹ and Claire Prigent-Combaret^{1*}

9

10 ¹ UMR Ecologie Microbienne, CNRS, INRA, VetAgro Sup, UCBL, Université de Lyon, 43
11 bd du 11 Novembre, F-69622 Villeurbanne, France

12

13 ² CNRS, INRA, UMR5004, Biochimie & Physiologie Moléculaire des Plantes, Montpellier,
14 France

15

16 # Current address: Université de Lausanne, Département de Microbiologie Fondamentale,
17 Quartier UNIL-Sorge, CH-1015 Lausanne, Switzerland

18

19

20

21 **Running title:** Root architecture effects of F113 on plants mostly involve the plant beneficial
22 functions encoded by *acdS* and *nirS* genes.

23

24

25 **Journal:** Molecular Plant-Microbe Interactions

26

27

28

29

30 ***Corresponding author:** Claire Prigent-Combaret, UMR CNRS 5557 Ecologie Microbienne,
31 Université Lyon 1, 43 bd du 11 Novembre 1918, 69622 Villeurbanne cedex, France. Phone:
32 +33 4 72 43 13 49. Fax: 33 4 72 43 12 23. E-mail: claire.prigent-combaret@univ-lyon1.fr

33 **SUMMARY**

34 Fluorescent pseudomonads are playing key roles in plant-bacteria symbiotic interactions due
 35 to the multiple plant-beneficial functions (PBFs) they are harboring. The relative
 36 contributions of PBFs to plant-stimulatory effects of the well-known PGPR *Pseudomonas*
 37 *kilonensis* F113 (formerly *P. fluorescens* F113) were investigated using a genetic approach.
 38 To this end, several deletion mutants were constructed: simple mutants $\Delta phlD$ (impaired in
 39 the biosynthesis of 2,4-diacetylphloroglucinol [DAPG]), $\Delta acdS$ (deficient in 1-
 40 aminocyclopropane-1-carboxylate [ACC] deaminase activity), Δgcd (glucose dehydrogenase
 41 deficient, impaired in phosphate solubilization), and $\Delta nirS$ (nitrite reductase deficient) and a
 42 quadruple mutant (deficient in the 4 PBFs mentioned above). Every PBF activity was
 43 quantified in the wild-type strain and the five deletion mutants. This approach revealed few
 44 functional interactions between PBFs *in vitro*. In particular, biosynthesis of glucose
 45 dehydrogenase severely reduced the production of DAPG. Contrariwise, the DAPG
 46 production impacted positively, but to a lesser extent, phosphate solubilization. Inoculation of
 47 the F113 wild-type strain on *Arabidopsis thaliana* Col-0 and maize seedlings modified the
 48 root architecture of both plants. Mutant strain inoculations revealed that the relative
 49 contribution of each PBF differed according to the measured plant traits, and that F113 plant-
 50 stimulatory effects did not correspond to the sum of each PBF relative contribution. Indeed,
 51 two PBF genes ($\Delta acdS$ and $\Delta nirS$) had a significant impact on root system architecture from
 52 both model plants, whether in *in vitro* and *in vivo* conditions. The current work underlined
 53 that few F113 PBFs seem to interact between each other in the free-living bacterial cells,
 54 whereas they control in concert *Arabidopsis thaliana* and maize growth and development.

55

56

57 **Key words:** co-occurring plant-beneficial functions, maize, *Arabidopsis*, functional
 58 interactions, fluorescent *Pseudomonas*

59

60 **INTRODUCTION**

61 Plant growth-promoting rhizobacteria (PGPR) are root-colonizing bacteria able to provide
62 growth and health benefits to plants through various mechanisms involving the expression of
63 plant-beneficial functions (PBFs) in PGPR (Bruto et al. 2014; Lemanceau et al. 2017;
64 Richardson et al. 2009; Vacheron et al. 2013). For example, PGPR can modulate plant
65 hormonal signalization by producing phytohormones such as auxins, cytokinins, gibberellins,
66 nitric oxide (NO) (Bashan and de-Bashan, 2010), or decreasing the emission of ethylene
67 (Glick et al. 1998; Honma and Shimomura, 1978; Vacheron et al. 2016a). PGPR may also
68 help plant nutrition by solubilizing inorganic compounds such as phosphate, or other mineral
69 elements (Adesemoye and Kloepper, 2009; Vessey, 2003). Finally, some PGPR, in particular
70 fluorescent pseudomonads, are producing antimicrobial compounds, such as 2,4-
71 diacetylphloroglucinol (DAPG), that protects plants against plant pathogen microorganisms
72 (Almario et al. 2014; Couillerot et al. 2009; Lanteigne et al. 2012) and activates plant
73 defenses (Iavicoli et al. 2003). Some of these antimicrobial compounds can also act as
74 communication signal between bacteria (Combes-Meynet et al. 2011).

75 The availability of an ever-increasing number of sequenced and annotated PGPR's
76 genomes is allowing us to perform some comparative genomic analyses (Flury et al. 2016;
77 Loper et al. 2012). The results of these analyses show the existence of combinations of PBF
78 genes that are specific to some PGPR taxa (Bruto et al. 2014). For example, in strains or
79 species belonging to the *Pseudomonas fluorescens* group, the genes required for the synthesis
80 of DAPG are present simultaneously with the ones required for cyanid hydrogen (HCN)
81 synthesis (Ramette et al. 2003). In *Pseudomonas protegens*, the production of pyoluteorin is
82 co-occurring with the production of DAPG (Ramette et al. 2011). The presence of co-
83 occurring PBF genes in genomes suggests that these functions might be part of common
84 bacterial regulatory or metabolic networks. Alternatively, Bashan and de-Bashan (2010)
85 hypothesized that each PBF present in one PGPR's genome would improve plant growth
86 either simultaneously or successively. In this additive hypothesis, the overall improvement of
87 plant growth would result from the sum of effects of each co-occurring PBF. Although the
88 relative contribution of several antimicrobial compounds to biocontrol performance has been
89 well studied (Calderón et al. 2013; Iavicoli et al. 2003; Romanowski et al. 2011; Voisard et al.
90 1989), the contribution of co-occurring PBFs in plant growth promotion is poorly
91 documented.

92 Among fluorescent pseudomonads, the *Pseudomonas kilonensis* F113 strain (formerly
 93 *Pseudomonas fluorescens*; Almario et al., 2017) is a PGPR strain isolated from sugar beet
 94 rhizosphere (Shanahan et al. 1992). That strain is well known for its biocontrol activity
 95 against a broad range of plant pathogen microorganisms (Cronin et al. 1997a; Cronin et al.
 96 1997b; Dunne et al. 1998). Less known, but all the more important, F113 also promotes plant
 97 growth and development, particularly on maize (Vacheron et al. 2016a; Walker et al. 2012),
 98 probably because of its rhizosphere's competence or in other words, its ability to efficiently
 99 colonize plant roots and to compete with other rhizosphere competent bacteria (Lugtenberg
 100 and Dekkers, 1999). The analysis of F113's genome sequence reveals the presence of multiple
 101 PBFs (Redondo-Nieto et al. 2013). We can identify the *phl* genes, which enable the
 102 production of DAPG (*phlD* encodes a polyketide synthase that is a key determinant of the
 103 DAPG biosynthesis), and also *gcd* encoding a glucose dehydrogenase involved in phosphate
 104 solubilization (Miller et al. 2010), *acdS* encoding the 1-aminocyclopropane-1-carboxylate
 105 (ACC) deaminase enzyme (Prigent-Combaret et al. 2008; Vacheron et al. 2016a) and *nirS*
 106 encoding the nitrite reductase involved in NO production (Choi et al. 2006). Specific
 107 associations of co-occurring PBFs were frequently observed among *Proteobacteria* (Bruto et
 108 al. 2014), and may reflect the existence of functional interactions occurring between PBFs. In
 109 F113, the interaction between the 4 PBFs (i.e. DAPG production, ACC deamination,
 110 phosphate solubilization, and NO production) may happen at a regulatory or metabolic level
 111 and could result, when combined altogether, in enhanced plant growth. Following the additive
 112 hypothesis, we predict that the 4 co-occurring PBFs exert additive beneficial effects on the
 113 development of plant root system architecture (RSA) and on the overall growth of plants by
 114 *P. kilonensis* F113. To test this hypothesis, we used a genetic approach and constructed 5
 115 mutant strains: 4 deleted for each PBFs, and one with deletion of the 4 PBFs. These 5 mutants
 116 were used to (i) analyze the functional relationships between F113 plant-beneficial activities
 117 and (ii) to determine if they are all equally contributing to the plant beneficial effects of F113
 118 on *Arabidopsis thaliana* in *in vitro* conditions, and on maize (*Zea mays* L.) in soil pot
 119 experiment.

120 RESULTS

121 ***In vitro*, most *P. kilonensis* F113's PBFs operate independently of each other**

122 The existence of functional interactions between the 4 co-occurring PBFs of *P. kilonensis*
 123 F113 was first tested *in vitro* and in absence of plants. In the wild-type F113 strain (WT) and

124 in each various mutant strains (i.e. $\Delta acdS$, $\Delta phlD$, $\Delta nirS$, Δgcd and the quadruple mutant
125 strain), we measured the activity of ACC deamination, phosphate solubilization, nitrite
126 reduction and DAPG synthesis. As expected, the deamination of ACC into α -ketobutyrate was
127 impaired in the $\Delta acdS$ and quadruple mutants (**Fig. 1A**). AcdS activity was weakly induced in
128 Δgcd and $\Delta nirS$ compared with F113 (1.7-fold and 1.3-fold respectively) and not significantly
129 affected in the $\Delta phlD$ mutant (**Fig. 1A**). Moreover, the insoluble phosphate was no longer
130 solubilized in the Δgcd and quadruple mutants (**Fig. 1B**). Furthermore, the glucose
131 dehydrogenase Gcd activity was weakly but significantly decreased (1.7-fold) in the $\Delta phlD$
132 mutant but remained identical to the one of F113 in $\Delta nirS$ and $\Delta acdS$ (**Fig. 1B**). The $\Delta nirS$
133 and the quadruple mutants were unable to reduce nitrite (and consequently to produce NO)
134 (**Fig. 1C**). The NirS activity in the $\Delta acdS$ or Δgcd or $\Delta phlD$ strain was identical to the one of
135 the F113 (**Fig. 1C**). As expected, there was no longer DAPG synthesis in the $\Delta phlD$ and
136 quadruple mutants (**Fig. 1D**). Interestingly, there was a strong accumulation of DAPG in the
137 Δgcd (82 times more than F113). By contrast the $\Delta acdS$ and $\Delta nirS$ produced as much DAPG
138 as F113 (**Fig. 1D**). Thus, the main functional interaction that occurs *in vitro* between all the
139 four different PBFs is between the cellular pathways containing the glucose dehydrogenase
140 Gcd and the polyketide synthase PhlD that both are involved in the control of DAPG
141 biosynthesis in *P. kilonensis* F113.

142 To further study the interaction between DAPG synthesis and the glucose
143 dehydrogenase, the DAPG production and phosphate solubilization were compared between
144 all double and triple deletion mutants (**Fig. S1**). On one hand, no phosphate solubilization was
145 observed in all *gcd* double and triple mutants. It is also significantly reduced in the
146 $\Delta phlD\Delta acdS$ (1.5-fold compared with F113), $\Delta phlD\Delta nirS$ (1.3-fold compared with F113),
147 and $\Delta phlD\Delta acdS\Delta nirS$ (1.7-fold compared with F113) mutants but in similar way than in the
148 single $\Delta phlD$ mutant (1.7-fold compared with F113). Thus, apart from the small positive
149 impact of DAPG production on the solubilization of phosphate, there is no other function that
150 interacts with the latter (**Fig. S1**). On the other hand, DAPG production is impaired in all *phlD*
151 double and triple mutants but is unaffected in a $\Delta acdS\Delta nirS$ mutant (**Fig. S1**). Compared to
152 the increase observed in a single *gcd* mutant (82 times higher than F113), DAPG production
153 is much more increased in a $\Delta acdS\Delta gcd$ mutant (226 times higher than F113) but reduced in
154 the $\Delta nirS\Delta gcd$ (30 times higher than F113) and $\Delta acdS\Delta gcd\Delta nirS$ mutants (26 times higher
155 than F113)(**Fig. S1**). These results show that the cellular network involving the glucose

156 dehydrogenase Gcd and the polyketide synthase PhlD is influenced negatively by *acdS* and
157 positively by *nirS* (**Fig. S1**).

158 **Deletion of PBF genes does not affect the fitness of *P. kilonensis* F113 *in vitro* but impair**
159 **its rhizosphere soil competitiveness**

160 When a PGPR does not enhance plant growth, it can be due to either from the absence of a
161 particular PBF in that strain, the poor expression of the PBF gene in the rhizosphere or to a
162 reduced rhizosphere competence. To assess if any of the tested PBF can affect rhizosphere
163 competence, we measured the growth of the WT strain and of every single and quadruple
164 mutant strains *in vitro* and *in vivo*. In liquid culture, bacterial growth can be limited by the
165 time required to divide (characterized by the growth rate) and the size of the cells population
166 in the stationary phase (characterized by the final OD reached in the liquid culture).

167 The growth rate of the quadruple mutant is higher than the one of the WT or any given
168 single mutant strain (**Fig. 2, Table S1**). The growth rates of all simple mutants are similar to
169 the one of the WT (**Fig. 2, Table S1**). In terms of final OD reached in stationary phase, the
170 quadruple and the $\Delta phlD$ mutants reached the highest optical density in the stationary growth
171 phase compared to any other single mutants and to the WT strain (**Fig. 2, Table S1**). Since
172 neither the $\Delta phlD$ nor the quadruple mutant do synthesize DAPG *in vitro* (**Fig. 1D**), these
173 results suggest that the production of DAPG might become toxic to F113 cells at the
174 stationary phase, in the tested conditions. To test that hypothesis, the growth of F113, $\Delta phlD$
175 and its complemented mutant was evaluated in presence or absence of DAPG (**Fig. S2**). First,
176 the complemented $\Delta phlD$ mutant had a growth kinetic curve similar to that of F113 (**Fig.**
177 **S2A**). Second, the addition of DAPG reduced significantly the optical density in the stationary
178 growth stage of F113 (starting from 0.1 $\mu\text{g}\cdot\text{ml}^{-1}$ of DAPG) (**Fig. S2B**). Third, the growth of
179 $\Delta phlD$ was slowed down in the exponential phase and reduced in the stationary growth by the
180 addition of DAPG at 0.5 $\mu\text{g}\cdot\text{ml}^{-1}$ and 1 $\mu\text{g}\cdot\text{ml}^{-1}$ (**Fig. S2C**). Fourth, the addition of DAPG (at
181 0.5 $\mu\text{g}\cdot\text{ml}^{-1}$ and 1 $\mu\text{g}\cdot\text{ml}^{-1}$) slowed down the exponential growth stage of the complemented
182 $\Delta phlD$ mutant, but the optical density reached in the stationary growth stage was quite similar
183 to that of the complemented $\Delta phlD$ mutant and of F113 (**Fig. S2D**). Thus, when DAPG
184 concentration reaches 0.5 $\mu\text{g}\cdot\text{ml}^{-1}$, it negatively affects the growth of F113. Although the *gcd*
185 mutant produced much more DAPG than the wild-type strain (and higher than 0.5 $\mu\text{g}\cdot\text{ml}^{-1}$), its
186 growth is nevertheless not affected. One can suggest that non-target effects of the *gcd*
187 mutation might result in protection of the bacterium against high DAPG concentration. In any

188 case, none of the simple and quadruple mutants have major deleterious effects on the F113
189 cell growth allowing us to analyze their role during the interaction of F113 with plant.

190 To monitor the contribution of PBF genes in the fitness of F113 in maize rhizosphere,
191 F113 and mutants were inoculated on maize seeds grown in natural soil, in presence of the
192 indigenous microbial communities. Same inoculation level of 5.10^6 bacteria per seed was
193 used for each strain. F113 cell population was stable up to 8 dpi (days post-inoculation), but
194 decreased at 20 dpi (**Fig. 3**). At 8 dpi, all mutant strains were found less abundant than F113
195 in the rhizosphere, the $\Delta phlD$ and quadruple mutants being the less numerous (**Fig. 3**). At 20
196 dpi, there was no significant difference in the rhizosphere colonization between F113 and the
197 $\Delta phlD$ and Δgcd mutants, whereas $\Delta acdS$, $\Delta nirS$ and the quadruple mutants were less
198 abundant than F113 (**Fig. 3**). Thus, all PBFs contribute to F113 rhizosphere competence but to
199 various extends. In particular, *phlD* is relevant for root colonization up to 8 days and *acdS* and
200 *nirS* genes are important for ensuring effective maize colonization over 20 days.

201 **The *acdS*, *nirS* and *gcd* genes affect maize growth**

202 F113 and PBF mutants were inoculated on maize seeds grown in pot filled with soil. Twenty
203 days after, shoot and root architecture traits were measured and the profiles obtained for each
204 strain were compared using hierarchical clustering analyses (HCA). Compared to the non-
205 inoculated condition, F113 significantly enhanced root growth (with an increase of total root
206 length of +50%, and of total root surface of +46%) and shoot growth (with an enhancement of
207 the total leaf surface of +44%) (**Tables S2, S3 and Fig. S3**).

208 When comparing the inoculation effects of mutants to that of F113 on maize by HCA,
209 two clusters were formed, grouping F113, $\Delta phlD$ and Δgcd on one hand and $\Delta acdS$, $\Delta nirS$
210 and the quadruple mutant in the other hand (**Fig. 4**). In the first cluster, all the plant
211 parameters appear evenly affected during inoculation, giving rise to a shape like a circle
212 similar to the one obtained with F113. It suggests that there are either no difference or minor
213 differences between F113 and the $\Delta phlD$ and Δgcd mutants. Consistent with that, there is no
214 significant differences between F113 and $\Delta phlD$ for all plant parameters assessed (**Table S2**
215 and **S3**), while the inoculation with Δgcd reduced significantly maize root length and surface
216 with respectively 26% and 20% of decrease compared to F113 (**Table S2**).

217 In the second cluster, the plant parameters appear to be unevenly affected, giving rise
218 to an unsymmetrical shape. The three strains belonging to that cluster (i.e. $\Delta acdS$, $\Delta nirS$ and
219 the quadruple mutant have a similar impact on maize development and growth (**Table S2** and

220 **S3**). Contrasting with the strains of the first cluster, the inoculation of $\Delta acdS$, $\Delta nirS$ and the
 221 quadruple mutant impacted significantly the root system architecture compared to F113 by
 222 reducing significantly the root length (-64%, -59% and -71%, respectively), the root surface (-
 223 50%, -50% and -57%, respectively), the number of root tips (respectively -62%; -45% and -
 224 71%) and the root fresh weight (respectively -31%, -38% and -42%) (**Table S2**). Thus, the
 225 RSA modifications triggered by F113 on maize were lost when $\Delta acdS$, $\Delta nirS$ or the quadruple
 226 mutants were inoculated (**Tables S2, S3** and **Fig. S3**).

227 In conclusion, F113's PBF genes and in particular *acdS* and *nirS* appear to alter mostly
 228 maize root parameters but not shoot parameters.

229 **F113 PBFs differently affect *A. thaliana* root hair elongation and primary root growth in** 230 **gnotobiotic agar conditions**

231 To further investigate what is F113's PBF impact on root, we turned to *in vitro* experiments,
 232 as they allow a careful monitoring of F113's effects on root development or root hairs for
 233 example. Because maize is a large plant, with a root system that is likely to be too large to be
 234 evaluated *in vitro*, we turned instead to *Arabidopsis*, as its root development shares some
 235 similarities with the one of maize (Atkinson *et al.*, 2014; Hochholdinger and Zimmermann,
 236 2008).

237 We first verified the effect of F113 inoculation and that of the various mutant strains
 238 on the *Arabidopsis* primary root growth. F113 inoculation inhibited significantly (2-fold) the
 239 primary root length of *A. thaliana* (**Fig. 5A**). When *A. thaliana* Col-0 was inoculated with
 240 $\Delta phlD$, a smaller reduction of the primary root growth (1.5-fold) compared to F113 was
 241 observed. However, the difference with F113 was not significant, implying that DAPG
 242 production only weakly contributed to the primary root length inhibition triggered by the WT
 243 strain (**Fig. 5A**). Contrarily, primary root length inhibition was lost when $\Delta acdS$, Δgcd , $\Delta nirS$
 244 or the quadruple mutants were inoculated (**Fig. 5A**). Therefore, *acdS*, *gcd* and *nirS*
 245 independently contribute to *Arabidopsis* primary root growth inhibition driven by F113 (**Fig.**
 246 **5A**). Secondly, we investigated the effect of F113 and of the various mutant strains on the
 247 plant root hair length. F113 inoculation led to significantly longer root hairs (**Fig. 5B**).
 248 Inoculation with the quadruple mutant generated the same plant phenotype than the non-
 249 inoculated condition, suggesting that at least one of the deleted PBFs was responsible of
 250 enhanced root hair length (**Fig. 5B**). However, compared to F113 WT inoculated plants, the
 251 average root hair lengths were significantly reduced by 20% in $\Delta phlD$, 14% in $\Delta acdS$, 21% in
 252 Δgcd inoculated plants, and up 41% in $\Delta nirS$ inoculated plants (**Fig. 5B**). Therefore, none of

253 F113's PBF functions is solely controlling root hair elongation. Because the activation of the
 254 plant ethylene signaling pathway results in root growth inhibition and root hair elongation
 255 (Pitts *et al.*, 1998; Swarup *et al.* 2007), and is also an indicator of the activation of a defense
 256 related mechanism (Broekgaarden *et al.*, 2015), we looked at the effects of F113 and of the
 257 various mutants strains on the plant ethylene emission by photoacoustic infra-red
 258 spectrophotometry (Cristescu *et al.*, 2012). Plant ethylene emissions increased significantly
 259 when F113 (1.5 fold), and $\Delta acdS$ (2 fold) were inoculated comparatively to the non-
 260 inoculated plant. The plant ethylene emission produced by $\Delta phlD$, Δgcd , $\Delta nirS$ and the
 261 quadruple mutant did not significantly differ from that of the non-inoculated condition (**Fig.**
 262 **6**). In conclusion, all F113's PBFs are contributing to the production of ethylene by
 263 *Arabidopsis*, but in a distinct manner: *acdS* is reducing *Arabidopsis* ethylene content whereas
 264 *phlD*, *gcd* and *nirS* are increasing it.

265 DISCUSSION

266 In this work, we evidence that interactions between PBFs might be different when bacteria are
 267 growing *in vitro* or in contact with a plant, where functional overlapping between PBFs may
 268 occur by affecting the same plant pathway. It highlights that inactivation of one PBF gene can
 269 affect the activity of other ones and that all PBFs harboured by PGPR have to be taken into
 270 account when analysing the plant response effects of PGPR inoculation.

271

272 Functional interactions between co-occurring PBFs in *P. kilonensis* F113

273 *In vitro*, the main functional interaction occurring in F113 cells between the four studied PBFs
 274 is between phosphate solubilization and biosynthesis of DAPG. We evidenced that the
 275 glucose dehydrogenase activity (*Gcd*) is repressing DAPG biosynthesis in F113 (**Fig. 1D**),
 276 confirming observations formerly made in *P. protegens* CHA0 (de Werra *et al.*, 2009). In
 277 cells containing a functional *Gcd*, glucose-6P is transformed into gluconic acid, which is
 278 exported out of the cells, leading to medium acidification and phosphate solubilization (**Fig.**
 279 **S4A**) (Stella and Halimi, 2015). When *gcd* is deleted, a higher quantity of glucose-6P could
 280 be provided to the glycolysis, resulting on the one hand in increased ATP production by the
 281 cell, and on the second hand in a higher amount of pyruvate that could then be incorporated to
 282 the tri-carboxylic acid cycle to produce higher amount of acetyl CoA, the precursor of DAPG
 283 (Bangera and Thomashow, 1999; Clifford *et al.* 2015) (**Fig. S4B**). Interestingly, a metabolic

284 interaction involving Gcd with another antimicrobial compound (i.e. pyoluteorin) has been
285 evidenced in *P. protegens* CHA0 (de Werra et al. 2009).

286 DAPG was shown to act as an intracellular messenger controlling transcription of
287 different PBFs genes such as pyoluteorin production in *P. protegens* CHA0 and Pf-5 (Clifford
288 et al. 2015; de Werra et al. 2011; Kidarsa et al. 2011; Schnider-Keel et al. 2000) or as an
289 intercellular messenger inducing PBFS in other PGPR as auxin production (Combes-Meynet
290 et al. 2011). Therefore, we hypothesize that the Δgcd mutant strain could also show some
291 specific modification at the transcriptional level of the expression of other PBFs encoding
292 genes, resulting in potential functional compensation.

293

294 **Distinct roles for F113 PBFs during colonization**

295 The functional importance of F113's PBF functions and its competitiveness against the native
296 soil populations of rhizobacteria was tested on maize plants growing in pot filled with non-
297 sterile soil, a setup close to natural conditions. For this experiment, we selected maize as a
298 model because it is frequently grown in fields where the soil we used has been collected
299 suggesting that this soil is enriched in a maize specific rhizosphere microbiota that is ideal to
300 compare the rhizosphere competitiveness of a mutant vs a wild-type strain. In addition, maize
301 plantlets have a large root system allowing an easy quantification of the colonization process.

302 Root secretion of organic substances is essential for the rhizosphere microbiota to
303 thrive (Haichar et al. 2016). Since the root exudates are composed of a lot of organic
304 molecules, which origin can be traced back to the photosynthetic activity of the plant, it is
305 important that the two time points selected to sample the maize root rhizosphere will not
306 differ in the physiological state of the plant. We sampled maize roots 8 days and 20 days after
307 sowing. In both case, the maize seedlings are already performing photosynthesis and may
308 release root exudate whose composition is not drastically dissimilar. Consistent with this
309 hypothesis, the composition in secondary metabolites present in root exudates from 5 distinct
310 maize inbred lines is less different between 8 and 10 days than it is between 3 and 5 days
311 post-germination (Walker and Prigent-Combaret, unpublished results).

312 At 8 dpi, there are less $\Delta phlD$ mutant bacteria in the maize root rhizosphere than F113
313 while at 20 dpi, the $\Delta phlD$ mutant strain is equally abundant as the WT (**Fig. 3**). This suggests
314 that DAPG is important at the beginning of the colonization process. DAPG is a well-known
315 antimicrobial compounds secreted by F113 (Cronin et al. 1997). Its secretion could limit the

316 presence of competitor rhizobacteria or fungi *in vivo*, hence favoring an exclusive interaction
 317 between F113 and the host roots. Curiously, the Δgcd mutant strain is equally abundant as the
 318 WT strain at both time points (**Fig. 3**). Yet, the Δgcd mutant strain produces 3 times more
 319 DAPG *in vitro* than the WT strain (**Fig. 1**). Enhanced DAPG production may trigger some
 320 compensation mechanisms in the Δgcd mutant strain, allowing it to colonize maize roots as
 321 efficiently as the wild-type strain.

322 At 20 dpi the colonization of the $\Delta nirS$, $\Delta acdS$ and the quadruple mutant is less
 323 efficient than that of F113, Δgcd , and $\Delta phlD$ (**Fig. 3**). $acdS^+$ strains are catabolizing ACC
 324 exuded by plant roots in α -ketobutyric acid (carbon source) and NH_4^+ (nitrogen source) (Glick
 325 et al. 1998). $acdS$ deletion can reduce the ability of F113 to fulfill its nutrient requirements in
 326 the rhizosphere, and thus its fitness and root colonization ability. NirS is allowing bacteria of
 327 the *Pseudomonas* genus, a strictly respiring genus, to respire NO_3^- and NO_2^- in the
 328 microaerophilic or anaerobic conditions that are frequently encountered in the rhizosphere
 329 (Højberg et al. 1999). Thus, the loss of nitrogen respiring capacity may explain the lower root
 330 colonization ability of the $\Delta nirS$ mutant that has previously been observed (Ghiglione et al.
 331 2002) as well as in our condition (**Fig. 3**). Since both NirS and AcdS are important for the
 332 colonization at 20 dpi, one could have expected that in the quadruple mutant strain, the effects
 333 of the two mutations would add up resulting in a strain with very poor ability to colonize at 20
 334 dpi. Surprisingly, this is not the case (**Fig. 3**). This suggests the existence of potential epistatic
 335 interactions between the two genes $nirS$ and $acdS$ or with gcd and/or $phlD$ that our *in vitro*
 336 analysis failed to unravel (**Fig. 1**). It also might be that plant exudates or microbe-microbe
 337 interactions in the rhizosphere result in activation of other genes that compensate for the lack
 338 of $nirS$ and $acdS$.

339 **The maize colonization process by F113 has a significant impact on the plant root and** 340 **shoot growth.**

341 To test if these different colonization patterns could affect maize growth *in vivo*, we measured
 342 15 different physiological parameters (8 for shoots and 7 for roots; **Table S2 and S3**). To get
 343 a broad view of the effect of F113 on maize plants, we have used a hierarchical clustering
 344 analysis (HCA). Instead of focusing on each parameter, HCA takes into account parameter
 345 patterns that can be compared between the mutant and the wild-type strains (**Fig. 4**). The
 346 inoculation of maize with the $\Delta phlD$ or Δgcd strains resulted in a pattern similar to the one of
 347 F113 (**Fig. 4**). Since $phlD$ appears to play a role for maize root colonization at 8 dpi (**Fig. 3**),
 348 it suggests that F113 colonization of maize roots after 8 dpi is more important for the effects

349 on maize growth than up to 8 dpi. Consistent with that interpretation, the inoculation of maize
 350 roots with the $\Delta nirS$ or $\Delta acdS$ or the quadruple mutant strain (all these genes are important for
 351 the colonization at 20 dpi (**Fig. 3**)), is resulting in a pattern different from the one of the WT
 352 (**Fig. 4**).

353 Contrasting with F113, inoculation with $\Delta acdS$ or $\Delta nirS$ or the quadruple mutant
 354 resulted in a decrease in total root length, total root surface and number of root tips while at
 355 the same time, an increase in root diameter (**Fig. 4, Table S2**). This indicates that *acdS* and
 356 *nirS*, two genes that are important for the fitness of F113, are also important for the root
 357 growth promotion. How they could be beneficial to root maize growth remains unclear. For
 358 example, it could be a direct interference with the plant ethylene pathway for *AcdS* or with
 359 the plant NO pathways for *NirS*. At the level of the shoot, maize plants inoculated with $\Delta acdS$
 360 or $\Delta nirS$ or the quadruple mutant show a weak decrease in leaf surfaces, as well as in
 361 chlorophyll content compared to F113 (**Fig. 4; Table S3**). While the leaf surface of inoculated
 362 maize plants by $\Delta acdS$, $\Delta nirS$ or the quadruple mutant are slightly higher than in the non-
 363 inoculated plants, the chlorophyll content is lower. As chlorophyll fluorescence is reduced in
 364 stressed plants (Bolh ar-Nordenkampf and  quist, 1993), this result could suggest that maize
 365 plants inoculated with $\Delta acdS$ or $\Delta nirS$ or the quadruple mutant are stressed, whereas F113
 366 may alleviate plant stress. Taken together, the PBF functions that contribute to the long-term
 367 fitness of F113 are also the ones that have the strongest effects on the growth of maize plants.

368 **Relative contribution of PBFs on *A. thaliana* root architecture**

369 To further study the contribution of the F113 various PBF's on the root development, we
 370 performed *in vitro* experiments with plants. We have used *Arabidopsis* as a model plant
 371 because it is small, it grows fast, it has a relatively simple root development program (tap
 372 root), and its root hairs are very easily observable. In addition, maize and *Arabidopsis* root
 373 development programs share some similarities (Atkinson *et al.*, 2014; Hochholdinger and
 374 Zimmermann, 2008). Finally, F113, which has been initially isolated from sugar beet roots is
 375 known to colonize efficiently both monocotyledons such as wheat (Couillerot *et al.* 2011; De
 376 La Fuente *et al.* 2006) and maize over more than 5 weeks (Couillerot *et al.* 2013; Von Felten
 377 *et al.* 2010) but also dicotyledonous crops such as alfalfa (Sanchez-Contreras *et al.* 2002;
 378 Villaceros *et al.* 2003) or tomato (de Weert *et al.* 2002).

379 *In vitro* F113 inoculation resulted in *Arabidopsis* primary root growth inhibition and
 380 strong promotion of root hair elongation (**Fig. 5A and B**). By contrast, the quadruple mutant
 381 showed no root architecture difference compared to the non-inoculated *Arabidopsis*,

382 suggesting that at least one F113 PBFs or a combination of PBFs may trigger root architecture
383 modifications (**Fig. 5, Fig. S3**). Several plant hormones such as auxin (controlling cell
384 division and elongation) (Spaepen and Vanderleyden, 2011) or ethylene (controlling root cell
385 elongation) (Jung and McCouch, 2013; Street et al. 2015; Swarup et al. 2007;) control
386 primary root elongation. However, F113 does not produce auxinic compounds (Vacheron,
387 Muller and Prigent-Combaret unpublished results) but instead is producing DAPG (**Fig. 1**).
388 One possibility is that DAPG could have an effect on the plant root system. Consistent with
389 this, when tomato seedlings are growing *in vitro* and in presence of 10 μ M DAPG, their
390 primary root growth is inhibited (Brazelton et al. 2008). However, the $\Delta phlD$ mutant (none
391 producing DAPG) remains able to inhibit *Arabidopsis* primary root elongation and the Δgcd
392 mutant (over-producing DAPG) does not show further reduced primary root length compared
393 to F113 (**Fig. 5**). In addition, both the $\Delta phlD$ and Δgcd mutants remain able to stimulate root
394 hair length. These results imply that, aside from DAPG, other F113 PBFs are involved in the
395 inhibition of the primary root elongation and stimulation of root hair length in *A. thaliana*.
396 Interestingly, the loss-of-function mutation in *nirS* affects the inhibition of primary root
397 growth (**Fig. 5A**), and the root hair elongation (**Fig. 5B**) significantly. This could suggest that
398 NO, produced by F113's NirS activity as evidenced by the use of the specific fluorescent
399 probe diaminorhodamine-4M acetoxymethyl ester (Vacheron, Muller and Prigent-Combaret
400 unpublished results), would act as an inhibitor of primary root growth and activator of root
401 hair elongation. Consistent with this, NO is described as a positive regulator of root hair
402 development (Lombardo et al. 2006; Lombardo and Lamattina, 2012) and a negative regulator
403 of primary root growth (Fernández-Marcos et al. 2011).

404 In absence of PGPR, plant ethylene is known to inhibit primary root length and to
405 activate root hairs elongation (Cao et al. 1999; Pitts et al. 1998). F113 moderately increased
406 plant ethylene emission, whereas all mutants but $\Delta acdS$, shared similar plant-ethylene
407 emission than non-inoculated condition (**Fig. 6**). Individually, each of the F113 PBFs
408 contributes positively to ethylene production by the plant during the associative symbiosis
409 with *A. thaliana* (**Fig. 6**). Contrasting with the other mutants, the $\Delta acdS$ strain colonization
410 results in higher ethylene emission by the plant (**Fig. 6**). Hence, the AcdS activity negatively
411 contributes to ethylene production. In our study, this mutant strain is the only one simple
412 mutant unable to degrade *in vitro* the ethylene precursor ACC (**Fig. 1A**). Assuming that the
413 mutant strain behaves similarly *in vitro* and *in vivo*, the lack of AcdS activity result in higher
414 ethylene emission by the plant (**Fig. 6**). However, this increase is not observed with the

415 inoculation of the quadruple mutant, showing that the other PBFs activate plant ethylene
 416 production. Thus, it confirms that F113 colonization of the root system results in modulation
 417 of ethylene emission by the plant and that AcdS is not the only one F113's PBF contributing
 418 to this effect. However, it remains to be seen if this emission is greater in the root, in the shoot
 419 or both plant organs. It also confirms that AcdS activity is actively decreasing plant ethylene
 420 emission during the associative symbiosis. This result is consistent with a long-standing
 421 hypothesis on the function of AcdS during its interaction with plants (Glick et al. 1998). Yet,
 422 this increased emission of ethylene in presence of the $\Delta acdS$ mutant strain does not result in a
 423 shorter primary and longer root hairs compared to the effect of the WT strain (**Fig. 5A**, and
 424 **B**). This absence of stronger root responses contrasts with previous observations suggesting
 425 that an absence of AcdS activity resulted in longer root hairs (Galland et al. 2012). But
 426 *Phyllobacterium brassicacearum* STM196, *Rhizobium leguminosarum* 128C53K and
 427 *Pseudomonas* sp. UW4, the strains used in that previous work, may not have the same
 428 combination of PBFs as the one of F113. Therefore, one should not rule out the possibility
 429 that this absence of stronger root responses with the $\Delta acdS$ strain is specific to F113 and its
 430 combination of PBFs. Another possibility that could explain the absence of stronger root
 431 responses, despite a significant increase in ethylene emission, is that F113 $\Delta acdS$ inoculated
 432 plants are becoming insensitive to the effect of high ethylene on root cells.

433 Taken together, F113 may trigger both ethylene-dependent and NO-dependent
 434 signalling pathways on *Arabidopsis*. Contrasting with the observations made on soil-pot
 435 grown maize, all F113's PBFs tested *in vitro* on *Arabidopsis* contribute to modification of the
 436 root architecture.

437

438 **EXPERIMENTAL PROCEDURES**

439

440 **Bacterial strains, plasmids and culture conditions**

441 The bacterial strains and plasmids used in this study are listed in (**Table S4**). *P. kilonensis*
 442 F113 wild-type and its mutants were incubated at 28°C in King's B broth media (Simon and
 443 Ridge, 1974) supplemented when required with gentamycin (15 $\mu\text{g}\cdot\text{ml}^{-1}$) or kanamycin (Km;
 444 50 $\mu\text{g}\cdot\text{ml}^{-1}$). *Escherichia coli* was incubated at 37°C in Luria Bertani broth (Bertani, 1951)
 445 supplemented with gentamycin (15 $\mu\text{g}\cdot\text{ml}^{-1}$) or ampicillin (75 $\mu\text{g}\cdot\text{ml}^{-1}$) and kanamycin (Km;
 446 50 $\mu\text{g}\cdot\text{ml}^{-1}$) when necessary. In order to assess the effects of DAPG on the growth of F113

447 and its mutants, DAPG (Santa Cruz Biotechnology, USA) was added in King's B broth
448 medium at 3 different concentrations (0.1 mg.ml⁻¹, 0.5 mg.ml⁻¹, and 1 mg.ml⁻¹).

449

450 **Growth kinetic assays**

451 Bacterial growth was monitored during 24 h at 28°C by measuring optical density (OD) in
452 a Bioscreen C analyzer (Labsystems, Finland) with one OD 600nm measured every 15 min.
453 Growth kinetic assays were performed three times independently with 5 technical repetitions.

454

455 **Construction of deletion mutants and complementation of the *phlD* deletion mutant**

456 To construct F113 PBF deletion mutants, about 700-pb fragments were amplified from
457 regions upstream and downstream the PBF genes of interest using specific primers (**Table S5**)
458 and subcloned into pGEM[®]-T easy (Promega, Madison, USA). The upstream and downstream
459 DNA fragments were digested with AatII/MunI and SacII/SacI for $\Delta phlD$ and Δgcd ,
460 AatII/PvuII and SacII/SacI for $\Delta acdS$, PvuII/MunI and SacII/SacI for $\Delta nirS$ and then cloned
461 one after another into pCM184, on both sides of the kanamycin resistance encoding gene
462 (Marx and Lidstrom, 2002). All restriction enzymes were supplied by ThermoFisher
463 Scientific (USA). All plasmid amplifications were done using *E. coli* JM109 chemically
464 competent cells (Promega, Madison, USA). For validation of the correct insertion of upstream
465 and downstream DNA fragments into pCM184, sequencing using primers S1F/S1R and
466 S2F/S2R was performed. pCM184 harboring upstream and downstream regions of the plant-
467 beneficial genes of interest were transformed into F113 by electroporation (Højberg et al.
468 1999). Inactivation mutants resulting from a double recombination event of upstream and
469 downstream regions were selected on King's B Km and screened for plant-beneficial gene
470 deletion by PCR with specific primers. Then, the plasmid CM157 containing the *cre-lox*
471 recombinase gene was introduced into F113 kanamycin resistant mutants in order to remove
472 the antibiotic marker. To check the loss of the kanamycin cassette, mutant strains were
473 screened for their inability to grow on King's B Km and by PCR using external primers. For
474 complementation of the *phlD* deletion mutant, the coding region of the *phlD* gene of F113
475 was amplified by PCR using primers phlDCompF1 and phlDCompR1 and subcloned into
476 pGEM-T easy. The *phlD* gene was extracted from pGEM-T easy using ApaI/SacI digestion
477 and inserted into the multiple cloning site of vector pBBR1MCS-5, under control of the lac

478 promoter, resulting in pBBR1-MCS5:*phlD*. This plasmid was introduced into the Δ *phlD*
479 mutant by electroporation (Højberg et al. 1999).

480

481 **DAPG quantification by HPLC**

482 DAPG production was measured by HPLC according to the method developed by (Bonsall et
483 al. 1997). Briefly, samples were analyzed with an Agilent 1200 series HPLC (Agilent
484 Technologies, Santa Carla, USA) equipped with a degasser (G132A), a quaternary pump
485 module (G1311A), an automatic sampler (G1329A) and a diode array detector (DAD
486 G1315B). Separation of compounds was performed at room temperature with a C18 reverse-
487 phase column. For each sample, 20 μ l were injected and eluted at 1 ml.min⁻¹ using a step-by-
488 step gradient increasing acetonitrile (ACN) proportion in water: the gradient started at 40% of
489 ACN over 4 min then rose from 40 to 64% in 7.5 min, then came to 75% at 16.5 min and
490 ended at 100% at 18.5min (100% maintained for 3 min before decreasing to 40% for 5 min).
491 Chromatograms were recorded at 270nm (maximum of absorbance of DAPG). The
492 chemstation Agilent software was used for integration of chromatograms, and quantitation of
493 DAPG was done according to a reference curve with the chemical standard (Sigma-Aldrich).
494 This experiment was done independently three times.

495

496 **ACC deaminase activity assay**

497 The ACC deaminase activity of strains was performed as described by Blaha et al. (2006).
498 The method is based on the quantification of α -ketobutyrate produced by the deamination of
499 ACC into α -ketobutyrate by the enzyme ACC deaminase. Total protein content in the assay
500 was measured using the BCA Protein Assay Kit (Pierce, Rockford, IL). ACC deaminase
501 activity was assessed three times for each strain. The data are expressed in nmol of
502 ketobutyrate.h⁻¹.mg of protein⁻¹. This experiment was done independently three times.

503

504 **Phosphate-solubilizing assay**

505 The phosphate-solubilizing ability of strains was evaluated by measuring tricalcium
506 phosphate solubilization halos on a National Botanical Research Institute's Phosphate
507 (NBRIP) agar medium. Strains were cultured for 1 day at 28°C in King's B broth and then
508 deposited 4 times (5 μ l each) on NBRIP agar medium. Solubilization halos were measured

509 after 6 days of incubation at 28°C using ImageJ software. This experiment was done three
510 times independently.

511

512 **Denitrification activity measurement**

513 The denitrification activity was estimated through the potential accumulation of N₂O in the
514 culture media, which is one step of the denitrification process. The accumulation of N₂O was
515 measured according to Bardon et al. (2016). Briefly, 20 ml of King's B media supplemented
516 with 20 mM of KNO₃ were placed in a plasma flask sealed by a rubber stopper. Anaerobic
517 condition was obtained removing air and replaced it with He/C₂H₂ mixture (90/10; v/v) in
518 order to inhibit the reduction of N₂O to N₂ and to allow the N₂O accumulation. Each strain
519 was inoculated at a final OD₆₀₀ of 0.1. N₂O emissions were measured every 2h during 24h
520 using gas chromatography coupled to a micro-katharometer detector (μGC-R3000, SRA
521 instruments, Marcy l'Etoile, France). The assay was performed twice with two technical
522 replicates. N₂O emission was expressed as μg of N-N₂O.h⁻¹.ml⁻¹ of media. In addition, the
523 ability of F113 to produce NO intracellularly was evaluated using the specific fluorescent
524 probe diaminorhodamine-4M acetoxymethyl ester (Calbiochem), as previously described by
525 Pothier et al. (2007).

526

527 **Bacterial inoculum preparation**

528 The *P. kilonensis* F113 wild-type and related deletion mutants $\Delta phlD$, $\Delta acdS$, Δgcd , $\Delta nirS$
529 and the quadruple mutant ($\Delta phlD\Delta acdS\Delta gcd\Delta nirS$) were incubated overnight at 28°C in
530 King's B broth medium. Cell cultures were centrifuged at 3000 rpm. The pellet was washed
531 with sterilized water and adjusted to 10⁷ bacteria.ml⁻¹.

532

533 **Bacterial inoculation effects on *Arabidopsis* root system architecture**

534 The seeds of *Arabidopsis thaliana* Ecotype Columbia0 (Col-0) were prepared according to
535 (Mantelin et al. 2006). After 7 days, plantlets were transferred to 50 ml of new plant agar
536 medium containing F113 or mutant strains at 10⁷ cells.ml⁻¹ in square Petri dishes (120 x 120
537 mm). Inoculated plantlets were transferred to a phytotron set to the following parameters:
538 21°C/days; 17°C/night, 13h light periods, 9500 lux. Four *Arabidopsis* plantlets were disposed
539 per Petri dish and 6 plates were prepared per condition. The 7 conditions tested were *A.*
540 *thaliana* inoculated with F113, with the 4 simple mutants, with the quadruple mutant and the

541 non-bacterized control condition. This experiment was made thrice independently. After 7
 542 days, 3 plants per Petri dishes were scanned in order to analyze the primary root elongation
 543 and root hair length using ImageJ software (i.e. 18 analyzed plants per condition). The relative
 544 contribution of each tested PBF in the modulation of the *Arabidopsis* root architecture was
 545 calculated as follow:

546 (1) F113 – control = α

547 (2) $((F113 - mutant) / \alpha) \times 100 =$ deleted gene relative contribution to F113 effect (%)

548

549 ***Arabidopsis* ethylene emission**

550 Measurements of *in vivo* ethylene emission by *Arabidopsis* plantlets were performed using
 551 infrared laser spectroscopy coupled to photo-acoustic detection (Cristescu et al. 2012) (ETD-
 552 300, SensorSense, Nijmegen, Holland). Practically, we carefully poured 600 μ l of sterile plant
 553 culture medium (as described above) inoculated or not with the various F113 strains at a final
 554 density of 2×10^7 cells.ml⁻¹ in a 2 ml sterile Eppendorf tube. Once solidified, we carefully
 555 introduced two wild-type *Arabidopsis* plantlets aged of seven days and closed the lid. Lids
 556 were punched to allow a regular breathing of the plants. This system was then transferred to a
 557 phytotron (MLR-352-PE, Panasonic, Gunma, Japan) set to the following parameters: 21°C
 558 (day); 17°C (night), 13h light period, 9500 lux. No measure was made during the first 48 h to
 559 allow plant acclimation, and in order to recover stress associated to the transfer. Prior ethylene
 560 emission measurement, 200 μ l of plant liquid medium was added in each tube in order to keep
 561 the head space humid, and therefore protecting the plant from the dry air coming from the
 562 compressed air bottle. Then, the lids of the tubes were removed and replaced by a rubber plug.
 563 Needles were pushed through the plug to allow the headspace to be flushed to the ethylene
 564 detector by compressed air. Every 90 min, the ethylene content in the headspace was
 565 measured while the tubes remained in the phytotron. That measurement was performed during
 566 two to three consecutive days to collect enough data on ethylene content during the day. At
 567 the end of the experiment, plant fresh weight was measured to allow data normalization. Raw
 568 results were exported into a spreadsheet in which they were normalized and processed to
 569 obtain at least 10 different measures of ethylene content in presence of light in each condition.

570

571 **Maize inoculation experiments in non-sterile soil**

572 The semi-late maize hybrid PR37Y15 (Pioneer Semences, Aussonne, France) was used in this
573 study. Maize seeds were surfaced disinfected. Briefly, seeds were soaked in sodium
574 hypochlorite (3.4%) during one hour with agitation. Five washes were performed with sterile
575 water. Four maize seeds were sown in non-sterile soil taken from La Côte Saint-André
576 (LCSA) near Lyon (France; Vacheron et al. 2016a) and placed in 2dm³ pots filled with 2.0kg
577 of sieved soil (5mm) with a water content of 20% (v/v). The moisture was maintained at 20%
578 during the experiment. Seeds (4 per pot) were inoculated with 100 µl of bacterial inoculum
579 solution, corresponding to 10⁶ bacteria. Ten pots per conditions were performed. Inoculum
580 impact on plant growth was assessed at 20 dpi by characterizing maize root system
581 architecture using WinRhizo (Reagent Instruments, Quebec City, Quebec, Canada). Leaf
582 surface was measured with the WinFolia image analysis software (Regent Instruments,
583 Quebec City, Quebec, Canada). Chlorophyll content was measured with a chlorophyll content
584 meter (Hansatech instruments model CL-01, Amesbury, USA). Root and shoot fresh and dry
585 biomasses were weighed. Ten plants were analyzed per conditions.

586

587 **Monitoring the bacterial maize root colonization**

588 The measurement of root colonization was assessed at 0, 8 and 20 dpi taking 10 seeds for
589 each condition at each sampling time. Inoculated seeds or plants were harvested and disposed
590 in a 50 ml Falcon tube and then soaked in liquid nitrogen. Seeds and root systems were
591 lyophilized and then scratched in order to extract DNA from the seed surface and root
592 adhering soil. DNA extractions from 500 mg of rhizosphere soils or seeds teguments were
593 performed using a FastDNATM SPIN Kit for Soil kit (MP Biomedicals, USA). DNA was also
594 extracted from 1 ml of inoculum solution in order to ascertain the cell concentration of the
595 inoculants. The seed and root bacterial colonization was assessed by real-time PCR as
596 described by Von Felten et al. (2010). Real-time PCR were performed using the
597 LightCycler® FastStart DNA Master SYBR® Green I kit and a LC-480 LightCycler (Roche
598 Applied Science, Indianapolis, IN). 5 ng of extracted DNA were used to assess the abundance
599 of seed and root colonization by the F113 parental and mutant strains using F113_1_for and
600 F113_1_rev primers with a detection limit of 10⁴ cells.seed⁻¹ and 10⁴ cells.g⁻¹ of rhizosphere
601 (Von Felten et al. 2010). Real-time PCR quantification data were converted to gene copy
602 number per gram of lyophilized root as described by Couillerot et al. (2012).

603

604 **Statistical analysis**

605 Regarding assays on each plant-beneficial function, data were log-transformed in order to
606 respect normal distribution and variances homogeneity and a one-way ANalysis Of VAriance
607 and Tukey's HSD tests were performed to detect significant differences between strains.
608 *Arabidopsis* root hair length data were compared using Kruskal-Wallis tests followed by post-
609 hoc non-parametric multiple comparisons. *Arabidopsis* primary root length data were square-
610 root transformed in order to respect variance homogeneity and normality and a one-way
611 ANOVA coupled with Tukey's HSD tests was performed. Ethylene emission data were
612 expressed related to non-inoculated condition and compared using ANOVA coupled with
613 Tukey's HSD tests. The comparison of root colonization between strains at the same sampling
614 time was analyzed by ANOVA and Tukey's HSD tests. The comparison of root colonization
615 across the time for each strain was analyzed by ANOVA and Fisher's LSD tests. The effects
616 of strain inoculation on maize growth parameters were compared using ANOVA and Tukey's
617 HSD tests and represented using star plot representation coupled to hierarchical clustering
618 analysis performed on the raw data (distance model: Euclidean; agglomeration method used:
619 UPGMA). All data were presented as mean \pm standard error. All analyses were performed at
620 $P < 0.05$, using R studio software (RStudio Team, 2015).

621

622 ACKNOWLEDGEMENTS

623 Jordan Vacheron was supported by a Ph.D grant from Academic Research Cluster 3 of
624 Rhône-Alpes Region. We thank M. Ribierre for technical help. We thank Sara Puijalon and
625 Vanessa Gardette from UMR CNRS 5023 for allowing us to use the Winfolia software. This
626 work made use of the 'Serre' technical platform of FR41 at Université Lyon 1 and the AME
627 platform (UMR 5557) for denitrification assays. We also thank Delphine Aymoz for English
628 proofreading of this paper. This study was supported by the ANR project SymbioMaize
629 (ANR-12-JSV7-0014-01).

630

631

632

633

634 REFERENCES

- 635 Adesemoye, A.O. and Kloepper, J.W. 2009. Plant–microbes interactions in enhanced fertilizer-use
636 efficiency. *Appl. Microbiol. Biotechnol.* 85:1–12.
- 637 Almario, J., Bruto, M., Vacheron, J., Prigent-Combaret, C., Moëgne-Loccoz, Y., and Muller, D.
638 2017. Distribution of 2, 4-Diacetylphloroglucinol biosynthetic genes among the
639 *Pseudomonas* spp. reveals unexpected polyphyletism. *Front. Microbiol.* 8:1218.
- 640 Almario, J., Muller, D., Défago, G., and Moëgne-Loccoz, Y. 2014. Rhizosphere ecology and
641 phytprotection in soils naturally suppressive to *Thielaviopsis* black root rot of tobacco.
642 *Environ. Microbiol.* 16:1949–1960.
- 643 Atkinson, J.A., Rasmussen, A., Traini, R., Voß, U., Sturrock, C., Mooney, S.J., Wells, D.M., and
644 Bennett, M.J. 2014. Branching out in roots: uncovering form, function, and regulation. *Plant*
645 *Physiol.* 166(2):538-550.
- 646 Baehler, E., Bottiglieri, M., Péchy-Tarr, M., Maurhofer, M., and Keel, C. 2005. Use of green
647 fluorescent protein-based reporters to monitor balanced production of antifungal compounds
648 in the biocontrol agent *Pseudomonas fluorescens* CHA0. *J. Appl. Microbiol.* 99:24–38.
- 649 Bangera, M.G. and Thomashow, L.S. 1999. Identification and characterization of a gene cluster for
650 synthesis of the polyketide antibiotic 2,4-diacetylphloroglucinol from *Pseudomonas*
651 *fluorescens* Q2-87. *J. Bacteriol.* 181:3155–3163.
- 652 Bardon, C., Piola, F., Haichar, F. el Z., Meiffren, G., Comte, G., Missery, B., et al. 2016.
653 Identification of B-type procyanidins in *Fallopia* spp. involved in biological denitrification
654 inhibition. *Environ. Microbiol.* 18:644–655.
- 655 Bashan, Y. and de-Bashan, L.E. 2010. Chapter two - How the plant growth-promoting bacterium
656 *Azospirillum* promotes plant growth—A critical assessment. In, *Advances in Agronomy*.
657 Academic Press, pp. 77–136.
- 658 Bertani, G. 1951. Studies on lyzogeny I. *J. Bacteriol.* 62:293–300.
- 659 Blaha, D., Prigent-Combaret, C., Mirza, M.S., and Moëgne-Loccoz, Y. 2006. Phylogeny of the 1-
660 aminocyclopropane-1-carboxylic acid deaminase-encoding gene *acdS* in phytobeneficial
661 and pathogenic Proteobacteria and relation with strain biogeography. *FEMS Microbiol.*
662 *Ecol.* 56:455–470.
- 663 Bolhår-Nordenkamp, H.R., and Öquist, G. 1993. Chlorophyll fluorescence as a tool in
664 photosynthesis research. In: *Photosynthesis and production in a changing environment: a*
665 *field and laboratory manual*; Hall, D. O., Scurlock, J.M.O., Bolhår-Nordenkamp, H.R.,
666 Leegood, R.C., and Long S.P. (Eds.); Chapman and Hall, London, United Kingdom, pp.
667 193-206.
- 668 Bonsall, R.F., Weller, D.M., and Thomashow, L.S. 1997. Quantification of 2,4-
669 diacetylphloroglucinol produced by fluorescent *Pseudomonas* spp. *in vitro* and in the
670 rhizosphere of wheat. *Appl. Environ. Microbiol.* 63:951–955.
- 671 Brazelton, J.N., Pfeufer, E.E., Sweat, T.A., Gardener, B.B.M., and Coenen, C. 2008. 2,4-
672 diacetylphloroglucinol alters plant root development. *Mol. Plant. Microbe Interact.*
673 21:1349–1358.
- 674 Broekgaarden, C., Caarls, L., Vos, I.A., Pieterse, C.M., Van Wees, S.C. 2015. Ethylene: traffic
675 controller on hormonal crossroads to defense. *Plant Physiol.* 169(4):2371-2379.
- 676 Bruto, M., Prigent-Combaret, C., Muller, D., and Moëgne-Loccoz, Y. 2014. Analysis of genes
677 contributing to plant-beneficial functions in plant growth-promoting rhizobacteria and
678 related Proteobacteria. *Sci. Rep.* 4:6261
- 679 Calderón, C.E., Pérez-García, A., de Vicente, A., and Cazorla, F.M. 2013. The *dar* genes of
680 *Pseudomonas chlororaphis* PCL1606 are crucial for biocontrol activity *via* production of the
681 antifungal compound 2-hexyl, 5-propyl resorcinol. *Mol. Plant. Microbe Interact.* 26:554–
682 565.

- 683 Cao, X.F., Linstead, P., Berger, F., Kieber, J., and Dolan, L. 1999. Differential ethylene sensitivity
684 of epidermal cells is involved in the establishment of cell pattern in the *Arabidopsis* root.
685 *Physiol. Plant.* 106:311–317.
- 686 Choi, P.S., Naal, Z., Moore, C., Casado-Rivera, E., Abruña, H.D., Helmann, J.D., and Shapleigh,
687 J.P. 2006. Assessing the impact of denitrifier-produced nitric oxide on other bacteria. *Appl.*
688 *Environ. Microbiol.* 72:2200–2205.
- 689 Clifford, J.C., Buchanan, A., Vining, O., Kidarsa, T.A., Chang, J.H., McPhail, K.L., and Loper, J.E.
690 2015. Phloroglucinol functions as an intracellular and intercellular chemical messenger
691 influencing gene expression in *Pseudomonas protegens*. *Environ. Microbiol.* 18:3296–3308.
- 692 Combes-Meynet, E., Pothier, J.F., Moëgne-Loccoz, Y., and Prigent-Combaret, C. 2011. The
693 *Pseudomonas* secondary metabolite 2,4-diacetylphloroglucinol is a signal inducing
694 rhizoplane expression of *Azospirillum* genes involved in plant-growth promotion. *Mol.*
695 *Plant. Microbe Interact.* 24:271–84.
- 696 Couillerot, O., Combes-Meynet, E., Pothier, J.F., Bellvert, F., Challita, E., Poirier, M.-A., et al.
697 2011. The role of the antimicrobial compound 2,4-diacetylphloroglucinol in the impact of
698 biocontrol *Pseudomonas fluorescens* F113 on *Azospirillum brasilense* phytostimulators.
699 *Microbiol. Read. Engl.* 157:1694–1705.
- 700 Couillerot, O., Prigent-Combaret, C., Caballero-Mellado, J., and Moëgne-Loccoz, Y. 2009.
701 *Pseudomonas fluorescens* and closely-related fluorescent pseudomonads as biocontrol
702 agents of soil-borne phytopathogens. *Lett. Appl. Microbiol.* 48:505–512.
- 703 Couillerot, O., Ramírez-Trujillo, A., Walker, V., von Felten, A., Jansa, J., Maurhofer, M., et al.
704 2013. Comparison of prominent *Azospirillum* strains in *Azospirillum-Pseudomonas-Glomus*
705 consortia for promotion of maize growth. *Appl. Microbiol. Biotechnol.* 97:4639–4649.
- 706 Cristescu, S.M., Mandon, J., Arslanov, D., Pessemier, J.D., Hermans, C., and Harren, F.J.M. 2012.
707 Current methods for detecting ethylene in plants. *Ann. Bot.* 111:347–360.
- 708 Cronin, D., Moëgne-Loccoz, Y., Fenton, A., Dunne, C., Dowling, D.N., and O’Gara, F. 1997a.
709 Ecological interaction of a biocontrol *Pseudomonas fluorescens* strain producing 2,4-
710 diacetylphloroglucinol with the soft rot potato pathogen *Erwinia carotovora* subsp.
711 *atroseptica*. *FEMS Microbiol. Ecol.* 23:95–106.
- 712 Cronin, D., Moëgne-Loccoz, Y., Fenton, A., Dunne, C., Dowling, D.N., and O’gara, F. 1997b. Role
713 of 2,4-diacetylphloroglucinol in the interactions of the biocontrol Pseudomonad strain F113
714 with the potato cyst nematode *Globodera rostochiensis*. *Appl. Environ. Microbiol.* 63:1357–
715 1361.
- 716 De La Fuente, L., Landa, B.B., and Weller, D.M. 2006. Host crop affects rhizosphere colonization
717 and competitiveness of 2,4-diacetylphloroglucinol-producing *Pseudomonas fluorescens*.
718 *Phytopathology* 96:751–762.
- 719 de Weert, S., Vermeiren, H., Mulders, I.H.M., Kuiper, I., Hendrickx, N., Bloemberg, G.V., et al.
720 2002. Flagella-driven chemotaxis towards exudate components is an important trait for
721 tomato root colonization by *Pseudomonas fluorescens*. *Mol. Plant. Microbe Interact.*
722 15:1173–1180.
- 723 de Werra, P. de, Huser, A., Tabacchi, R., Keel, C., and Maurhofer, M. 2011. Plant- and microbe-
724 derived compounds affect the expression of genes encoding antifungal compounds in a
725 Pseudomonad with biocontrol activity. *Appl. Environ. Microbiol.* 77:2807–2812.
- 726 de Werra, P., Péchy-Tarr, M., Keel, C., and Maurhofer, M. 2009. Role of gluconic acid production
727 in the regulation of biocontrol traits of *Pseudomonas fluorescens* CHA0. *Appl. Environ.*
728 *Microbiol.* 75:4162–4174.
- 729 Dunne, C., Moëgne-Loccoz, Y., McCarthy, J., Higgins, P., Powell, J., Dowling, D.N., and O’Gara,
730 F. 1998. Combining proteolytic and phloroglucinol-producing bacteria for improved
731 biocontrol of Pythium-mediated damping-off of sugar beet. *Plant Pathol.* 47:299–307.
- 732 Fernández-Marcos, M., Sanz, L., Lewis, D.R., Muday, G.K., and Lorenzo, O. 2011. Nitric oxide
733 causes root apical meristem defects and growth inhibition while reducing PIN-FORMED 1

- 734 (PIN1)-dependent acropetal auxin transport. Proc. Natl. Acad. Sci. U. S. A. 108:18506–
735 18511.
- 736 Flury, P., Aellen, N., Ruffner, B., Péchy-Tarr, M., Fataar, S., Metla, Z., et al. 2016. Insect
737 pathogenicity in plant-beneficial pseudomonads: phylogenetic distribution and comparative
738 genomics. ISME J. 10:2527-2542
- 739 Galland, M., Gamet, L., Varoquaux, F., Touraine, B., Touraine, B., and Desbrosses, G. 2012. The
740 ethylene pathway contributes to root hair elongation induced by the beneficial bacteria
741 *Phyllobacterium brassicacearum* STM196. Plant Sci. 190:74–81.
- 742 Ghiglione, J.-F., Richaume, A., Philippot, L., and Lensi, R. 2002. Relative involvement of nitrate
743 and nitrite reduction in the competitiveness of *Pseudomonas fluorescens* in the rhizosphere
744 of maize under non-limiting nitrate conditions. FEMS Microbiol. Ecol. 39:121–127.
- 745 Glick, B.R., Penrose, D.M., and Li, J. 1998. A model for the lowering of plant ethylene
746 concentrations by plant growth-promoting bacteria. J. Theor. Biol. 190:63–68.
- 747 Haichar, Z.F., Heulin, T., Guyonnet, J. P., and Achouak, W. 2016. Stable isotope probing of carbon
748 flow in the plant holobiont. Curr. Opin. Biotechnol. 41:9–13.
- 749 Hochholdinger, F., Zimmermann R. 2008. Conserved and diverse mechanisms in root development.
750 Curr. Opin. Plant Biol. 11(1):70-74.
- 751 Højberg, O., Schnider, U., Winteler, H.V., Sørensen, J., and Haas, D. 1999. Oxygen-sensing
752 reporter strain of *Pseudomonas fluorescens* for monitoring the distribution of low-oxygen
753 habitats in soil. Appl. Environ. Microbiol. 65:4085–4093.
- 754 Honma, M. and Shimomura, T. 1978. Metabolism of 1-aminocyclopropane-1-carboxylic acid.
755 Agric. Biol. Chem. 42:1825–1831.
- 756 Iavicoli, A., Boutet, E., Buchala, A., and Métraux, J.-P. 2003. Induced systemic resistance in
757 *Arabidopsis thaliana* in response to root inoculation with *Pseudomonas fluorescens* CHA0.
758 Mol. Plant. Microbe Interact. 16:851–858.
- 759 Jung, J.K.H. and McCouch, S. 2013. Getting to the roots of it: genetic and hormonal control of root
760 architecture. Front. Plant Genet. Genomics 4:186.
- 761 Kidarsa, T.A., Goebel, N.C., Zabriskie, T.M., and Loper, J.E. 2011. Phloroglucinol mediates
762 cross-talk between the pyoluteorin and 2,4-diacetylphloroglucinol biosynthetic pathways
763 in *Pseudomonas fluorescens* Pf-5. Mol. Microbiol. 81:395–414.
- 764 Lanteigne, C., Gadkar, V.J., Wallon, T., Novinscak, A., and Fillion, M. 2012. Production of DAPG
765 and HCN by *Pseudomonas* sp. LBUM300 contributes to the biological control of bacterial
766 canker of tomato. Phytopathology 102:967–973.
- 767 Leij, F.A.D., Dixon-Hardy, J.E., and Lynch, J.M. 2002. Effect of 2,4-diacetylphloroglucinol-
768 producing and non-producing strains of *Pseudomonas fluorescens* on root development of
769 pea seedlings in three different soil types and its effect on nodulation by *Rhizobium*. Biol.
770 Fertil. Soils 35:114–121.
- 771 Lemanceau, P., Blouin, M., Muller, D., and Moëgne-Loccoz, Y. 2017. Let the core microbiota be
772 functional. Trends Plant Sci. 22:583-595.
- 773 Lombardo, M.C., Graziano, M., Polacco, J.C., and Lamattina, L. 2006. Nitric oxide functions as a
774 positive regulator of root hair development. Plant Signal. Behav. 1:28–33.
- 775 Lombardo, M.C. and Lamattina, L. 2012. Nitric oxide is essential for vesicle formation and
776 trafficking in *Arabidopsis* root hair growth. J. Exp. Bot. 63:4875-85
- 777 Loper, J.E., Hassan, K.A., Mavrodi, D.V., Davis, E.W., Lim, C.K., Shaffer, B.T., et al. 2012.
778 Comparative genomics of plant-associated *Pseudomonas* spp.: insights into diversity and
779 inheritance of traits involved in multitrophic interactions. PLoS Genet. 8:e1002784.
- 780 Lugtenberg B.J.J., Dekkers L.C. 1999. What makes *Pseudomonas* bacteria rhizosphere competent?
781 Environ. Microbiol. 1:9–13.
- 782 Ma, Z., Hua, G.K.H., Ongena, M., and Höfte, M. 2016. Role of phenazines and cyclic lipopeptides
783 produced by *Pseudomonas* sp. CMR12a in induced systemic resistance on rice and bean.
784 Environ. Microbiol. Rep. 8:896–904.

- 785 Mantelin, S., Desbrosses, G., Larcher, M., Tranbarger, T.J., Cleyet-Marel, J.-C., and Touraine, B.
786 2006. Nitrate-dependent control of root architecture and N nutrition are altered by a plant
787 growth-promoting *Phyllobacterium* sp. *Planta* 223:591–603.
- 788 Marx, C.J. and Lidstrom, M.E. 2002. Broad-host-range cre-lox system for antibiotic marker
789 recycling in gram-negative bacteria. *Biotechniques* 33:1062–1067.
- 790 Meyer, J.B., Frapolli, M., Keel, C., and Maurhofer, M. 2011. Pyrroloquinoline quinone biosynthesis
791 gene *pqqC*, a novel molecular marker for studying the phylogeny and diversity of
792 phosphate-solubilizing pseudomonads. *Appl. Environ. Microbiol.* 77:7345–7354.
- 793 Miller, S.H., Browne, P., Prigent-Combaret, C., Combes-Meynet, E., Morrissey, J.P., and O’Gara,
794 F. 2010. Biochemical and genomic comparison of inorganic phosphate solubilization in
795 *Pseudomonas* species. *Environ. Microbiol. Rep.* 2:403–411.
- 796 Moëgne-Loccoz, Y., Powell, J., Higgins, P., McCarthy, J., and O’Gara, F. 1998. An investigation of
797 the impact of biocontrol *Pseudomonas fluorescens* F113 on the growth of sugarbeet and the
798 performance of subsequent clover-Rhizobium symbiosis. *Appl. Soil Ecol.* 7:225–237.
- 799 Penrose, D.M. and Glick, B.R. 2003. Methods for isolating and characterizing ACC deaminase-
800 containing plant growth-promoting rhizobacteria. *Physiol. Plant.* 118:10–15.
- 801 Pitts, R.J., Cernac, A., and Estelle, M. 1998. Auxin and ethylene promote root hair elongation in
802 *Arabidopsis*. *Plant J. Cell Mol. Biol.* 16:553–560.
- 803 Pothier, J.F., Wisniewski-Dyé, F., Weiss-Gayet, M., Moëgne-Loccoz, Y., and Prigent-Combaret, C.
804 2007. Promoter trap identification of wheat seed extract-induced genes in the plant-growth-
805 promoting rhizobacterium *Azospirillum brasilense* Sp245. *Microbiology.* 153:3608-3622.
- 806 Prigent-Combaret, C., Blaha, D., Pothier, J.F., Vial, L., Poirier, M.-A., Wisniewski-Dyé, F., and
807 Moëgne-Loccoz, Y. 2008. Physical organization and phylogenetic analysis of *acdR* as
808 leucine-responsive regulator of the 1-aminocyclopropane-1-carboxylate deaminase gene
809 *acdS* in phytobeneficial *Azospirillum lipoferum* 4B and other Proteobacteria. *FEMS*
810 *Microbiol. Ecol.* 65:202–219.
- 811 Ramette, A., Moëgne-Loccoz, Y., and Défago, G. 2003. Prevalence of fluorescent pseudomonads
812 producing antifungal phloroglucinols and/or hydrogen cyanide in soils naturally suppressive
813 or conducive to tobacco black root rot. *FEMS Microbiol. Ecol.* 44:35–43.
- 814 Ramette, A., Frapolli, M., Fischer-Le Saux, M., Gruffaz, C., Meyer, J.M., Défago, G., Sutra, L.,
815 Moëgne-Loccoz, Y. 2011. *Pseudomonas protegens* sp. nov., widespread plant-protecting
816 bacteria producing the biocontrol compounds 2,4-diacetylphloroglucinol and pyoluteorin.
817 *Syst. Appl. Microbiol.* 34:180-188.
- 818 Redondo-Nieto, M., Barret, M., Morrissey, J., Germaine, K., Martínez-Granero, F., Barahona, E., et
819 al. 2013. Genome sequence reveals that *Pseudomonas fluorescens* F113 possesses a large
820 and diverse array of systems for rhizosphere function and host interaction. *BMC Genomics*
821 14:54.
- 822 Richardson, A.E., Barea, J.-M., McNeill, A.M., and Prigent-Combaret, C. 2009. Acquisition of
823 phosphorus and nitrogen in the rhizosphere and plant growth promotion by microorganisms.
824 *Plant Soil* 321:305–339.
- 825 Romanowski, A., Migliori, M.L., Valverde, C., and Golombek, D.A. 2011. Circadian variation in
826 *Pseudomonas fluorescens* (CHA0)-mediated paralysis of *Caenorhabditis elegans*. *Microb.*
827 *Pathog.* 50:23–30.
- 828 RStudio Team. 2015. RStudio: Integrated Development for R. RStudio, Inc., Boston, MA.
- 829 Sanchez-Contreras, M., Martin, M., Villaceros, M., O’Gara, F., Bonilla, I., and Rivilla, R. 2002.
830 Phenotypic selection and phase variation Occur during Alfalfa root colonization by
831 *Pseudomonas fluorescens* F113. *J. Bacteriol.* 184:1587–1596.
- 832 Schnider-Keel, U., Seematter, A., Maurhofer, M., Blumer, C., Duffy, B., Gigot-Bonnefoy, C., et al.
833 2000. Autoinduction of 2,4-diacetylphloroglucinol biosynthesis in the biocontrol agent
834 *Pseudomonas fluorescens* CHA0 and repression by the bacterial metabolites salicylate and
835 pyoluteorin. *J. Bacteriol.* 182:1215–1225.

- 836 Shanahan, P., O'Sullivan, D.J., Simpson, P., Glennon, J.D., and O'Gara, F. 1992. Isolation of 2,4-
837 diacetylphloroglucinol from a fluorescent *Pseudomonas* and investigation of physiological
838 parameters influencing its production. *Appl. Environ. Microbiol.* 58:353–358.
- 839 Simon, A. and Ridge, E.H. 1974. The use of ampicillin in a simplified selective medium for the
840 isolation of fluorescent pseudomonads. *J. Appl. Bacteriol.* 37: 459–460.
- 841 Spaepen, S. and Vanderleyden, J. 2011. Auxin and plant-microbe interactions. *Cold Spring Harb.*
842 *Perspect. Biol.* 3: a001438.
- 843 Stella, M. and Halimi, M.S. 2015. Gluconic acid production by bacteria to liberate phosphorus from
844 insoluble phosphate complexes. *J. Trop. Agric. Fd. Sc.* 43:41– 53.
- 845 Street, I.H., Aman, S., Zubo, Y., Ramzan, A., Wang, X., Shakeel, S.N., et al. 2015. Ethylene
846 inhibits cell proliferation of the *Arabidopsis* root meristem. *Plant Physiol.* 169:338–350.
- 847 Swarup, R., Perry, P., Hagenbeek, D., Straeten, D.V.D., Beemster, G.T.S., Sandberg, G., et al.
848 2007. Ethylene upregulates auxin biosynthesis in *Arabidopsis* seedlings to enhance
849 inhibition of root cell elongation. *Plant Cell* 19:2186–2196.
- 850 Vacheron, J., Combes-Meynet, E., Walker, V., Gouesnard, B., Muller, D., Moëgne-Loccoz, Y., and
851 Prigent-Combaret, C. 2016a. Expression on roots and contribution to maize
852 phytostimulation of 1-aminocyclopropane-1-decarboxylate deaminase gene *acdS* in
853 *Pseudomonas fluorescens* F113. *Plant Soil.* 407:187–202.
- 854 Vacheron, J., Desbrosses, G., Bouffaud, M.-L., Touraine, B., Moëgne-Loccoz, Y., Muller, D., et al.
855 2013. Plant growth-promoting rhizobacteria and root system functioning. *Front. Plant Sci.*
856 4:356.
- 857 Vacheron, J., Moëgne-Loccoz, Y., Dubost, A., Gonçalves-Martins, M., Muller, D., and Prigent-
858 Combaret, C. 2016b. Fluorescent *Pseudomonas* strains with only few plant-beneficial
859 properties are favored in the maize rhizosphere. *Front. Plant Sci.* 7:1212.
- 860 Vessey, J.K. 2003. Plant growth promoting rhizobacteria as biofertilizers. *Plant Soil* 255:571–586.
- 861 Villacieros, M., Power, B., Sánchez-Contreras, M., Lloret, J., Oruezabal, R.I., Martín, M., et al.
862 2003. Colonization behaviour of *Pseudomonas fluorescens* and *Sinorhizobium meliloti* in
863 the alfalfa (*Medicago sativa*) rhizosphere. *Plant Soil* 251:47–54.
- 864 Voisard, C., Keel, C., Haas, D., and Défago, G. 1989. Cyanide production by *Pseudomonas*
865 *fluorescens* helps suppress black root rot of tobacco under gnotobiotic conditions. *EMBO J.*
866 8:351–358.
- 867 Von Felten, A., Défago, G., and Maurhofer, M. 2010. Quantification of *Pseudomonas fluorescens*
868 strains F113, CHA0 and Pfl53 in the rhizosphere of maize by strain-specific real-time PCR
869 unaffected by the variability of DNA extraction efficiency. *J. Microbiol. Methods* 81:108–
870 115.
- 871 Walker, V., Couillerot, O., Felten, A.V., Bellvert, F., Jansa, J., Maurhofer, M., et al. 2012. Variation
872 of secondary metabolite levels in maize seedling roots induced by inoculation with
873 *Azospirillum*, *Pseudomonas* and *Glomus* consortium under field conditions. *Plant Soil*
874 356:151–163.
- 875
- 876

877 **FIG. LEGENDS**

878

879 **Fig.1: Effect of the deletion of F113 plant beneficial functions (PBFs) on each PBF activity of**
 880 **the strain.** A: 1-aminocyclopropane-1-carboxylate (ACC) deaminase activity; B: Phosphate
 881 solubilization assay; C: N₂O quantification; D: 2,4-diacetylphloroglucinol (DAPG) quantification.
 882 ND: non-detected. Statistical differences between strains for each tested PBF are indicated with
 883 letter a-c. (ANOVA and Tukey's HSD test, $P < 0.05$). Absence of letter indicates that differences
 884 were not significant.

885

886 **Fig. 2: Growth curve of the *P. kilonensis* F113 and its PBF mutants in King's B broth at 28°C.**
 887 The data represent the means of five replicate cultures (standard errors were not presented but lower
 888 than 10%). The experiment was done three times independently.

889 **Fig. 3: Comparison of maize root colonization levels between *P. kilonensis* F113 and its PBF**
 890 **mutants.** The grey color corresponds to root colonization at the moment of the seed inoculation
 891 (day 0), dark at 8 dpi and white at 20 dpi. Statistical differences across the time are represented with
 892 letters A-C. Statistical differences between strains at a given time are represented with letters a-c.
 893 The dotted line corresponds to the qPCR detection limit. NI: Non-inoculated condition.

894

895 **Fig. 4: Comparison of the effects of *P. kilonensis* F113 PBF mutants on maize growth by**
 896 **hierarchical clustering.** For each plant parameters, ratio between data obtained with mutants and
 897 with F113 were calculated and expressed in percent. Root and shoot measured parameters are
 898 colored respectively in brown and green on the star plot. LS#1: surface of the leaf number 1 (same
 899 nomenclature for leaf 2 and 3); LSTot: Total leaf surface; Chl: Chlorophyll content in leaf number
 900 3; FSM: Fresh shoot mass; DSM: Dry shoot mass. L: total root length, S: Total root surface; D:
 901 Root diameter; V: root volume; T: Root tips; FRM: Fresh root mass; DRM: Dry root mass. R/S
 902 represents the ratio between the dry root biomass and the dry shoot biomass. Raw data were
 903 processed through hierarchical clustering analysis using Euclidean model and UPGMA as
 904 agglomeration method.

905

906 **Fig. 5: Effects of the inoculation of *P. kilonensis* F113 and its PBF mutants on the length of**
 907 ***Arabidopsis* primary roots (A) and root hairs (B).** NI: Non-inoculated condition. Conditions
 908 harboring the same letter were not significantly different (ANOVA, Tukey's HSD test, $P < 0.05$).

909

910 **Fig. 6: Plant ethylene emission in response to the inoculation of *Arabidopsis* plantlets with *P.***
911 ***kilonensis* F113 and its PBF mutants.** Plant ethylene emission was calculated related to the plant
912 ethylene emission for the non-inoculated condition (NI). Conditions harboring the same letter were
913 not significantly different (ANOVA, Tukey's HSD test, $P < 0.05$).

914

915

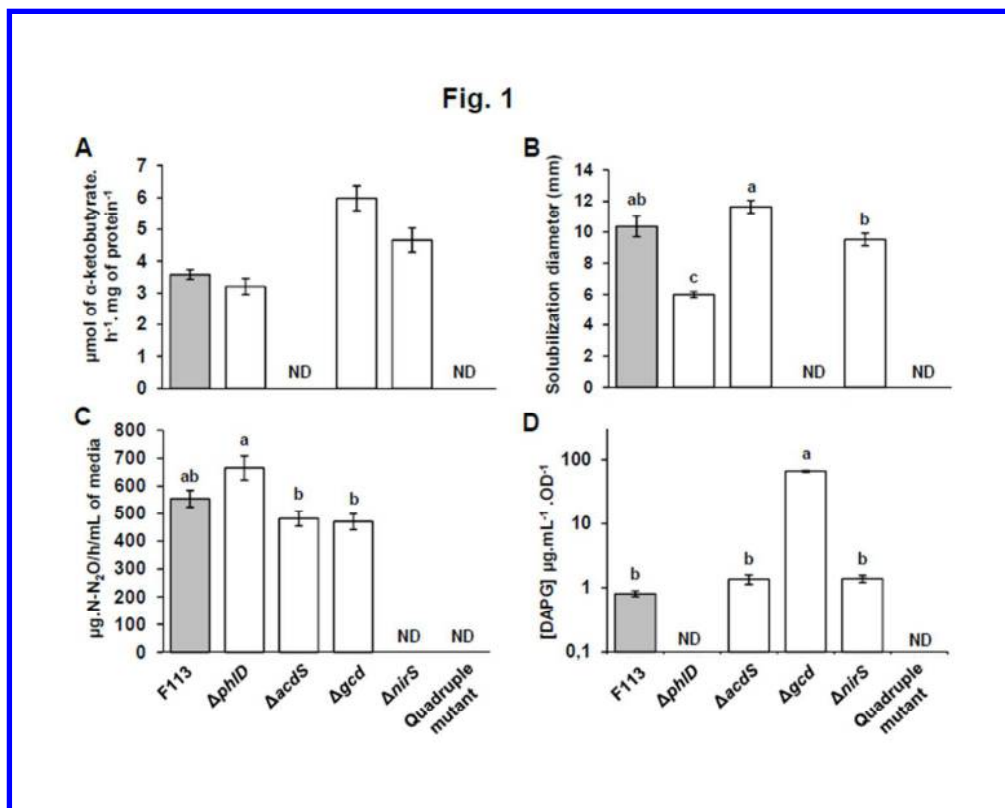


Fig. 1

281x222mm (72 x 72 DPI)

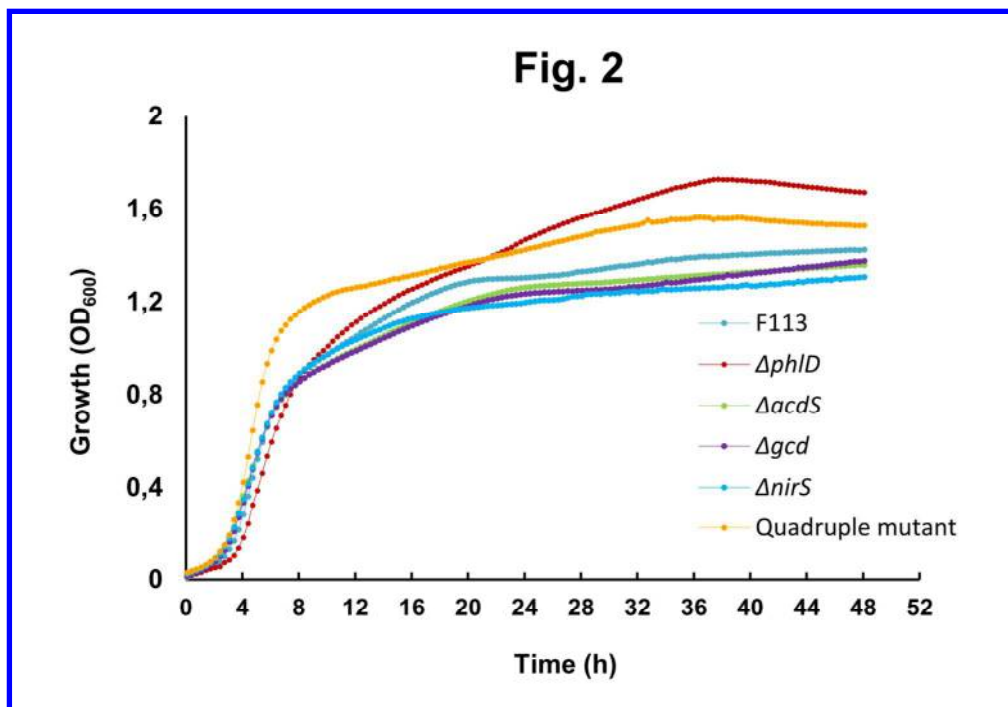


Fig. 2

132x91mm (300 x 300 DPI)

Comment citer ce document :

Vacheron, J., Desbrosses, G., Renoud, S., Padilla-Aguilar, R.-M., Walker, V., Muller, D., prigent-combaret, c. (Auteur de correspondance) (2018). Differential contribution of plant-beneficial functions from *Pseudomonas kilonensis* F113 to root system architecture alterations in *Arabidopsis thaliana* and *Zea mays*. *Molecular Plant-Microbe Interactions*. 31 (2). 212-223. . DOI :

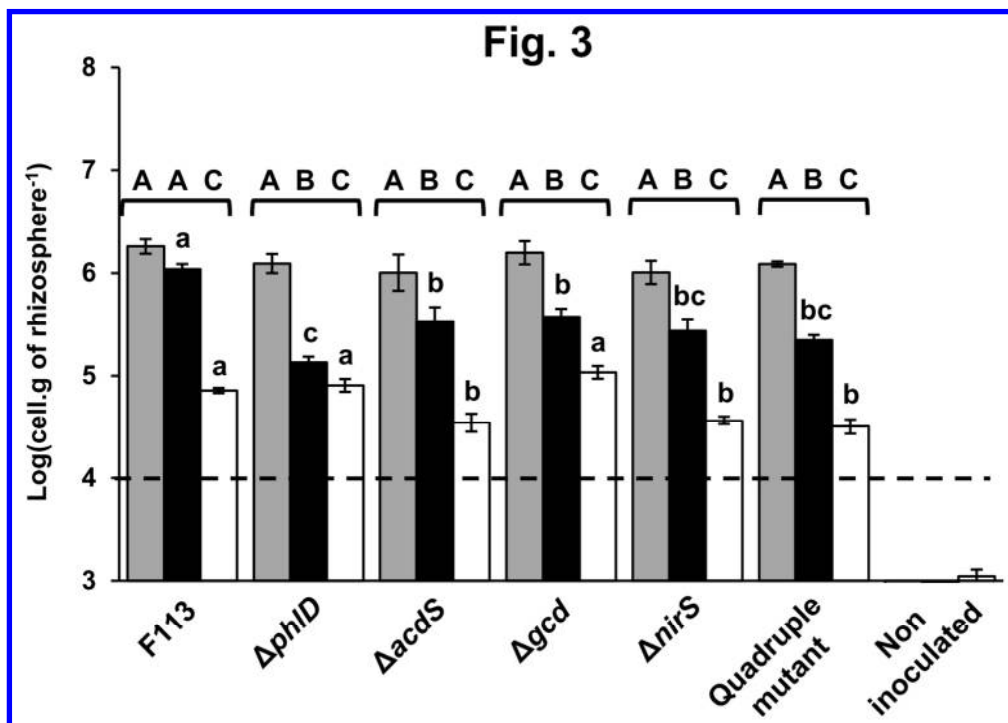


Fig. 3

133x94mm (300 x 300 DPI)

Comment citer ce document :

Vacheron, J., Desbrosses, G., Renoud, S., Padilla-Aguilar, R.-M., Walker, V., Muller, D., prigent-combaret, c. (Auteur de correspondance) (2018). Differential contribution of plant-beneficial functions from *Pseudomonas kilonensis* F113 to root system architecture alterations in *Arabidopsis thaliana* and *Zea mays*. *Molecular Plant-Microbe Interactions*. 31 (2). 212-223. DOI :

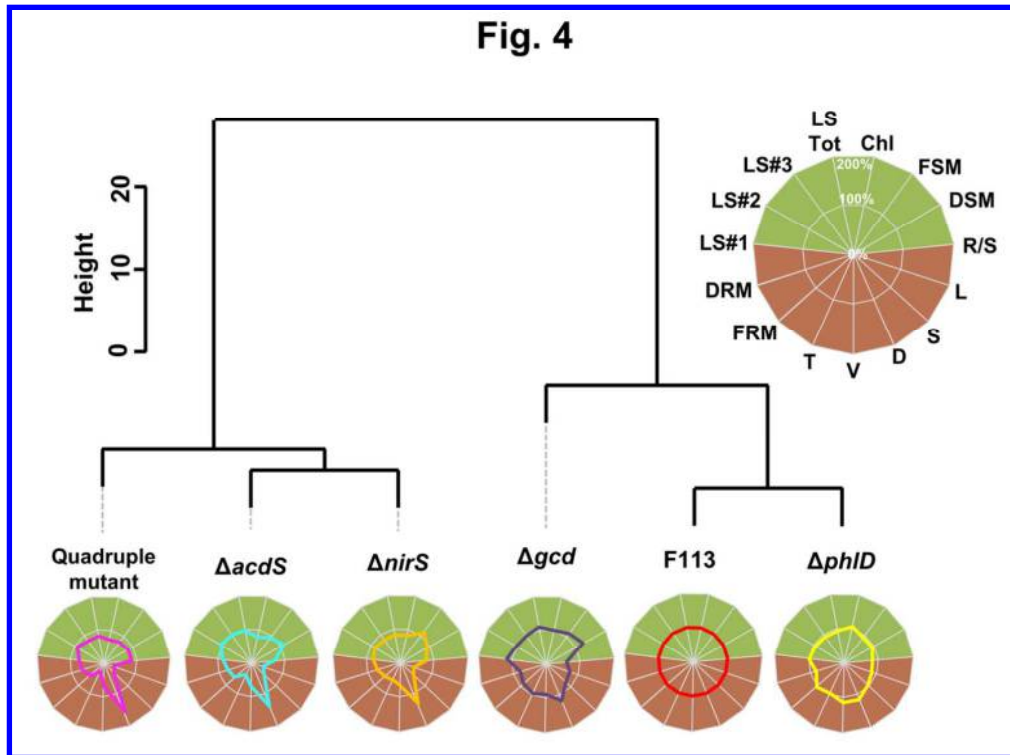


Fig. 4

112x83mm (300 x 300 DPI)

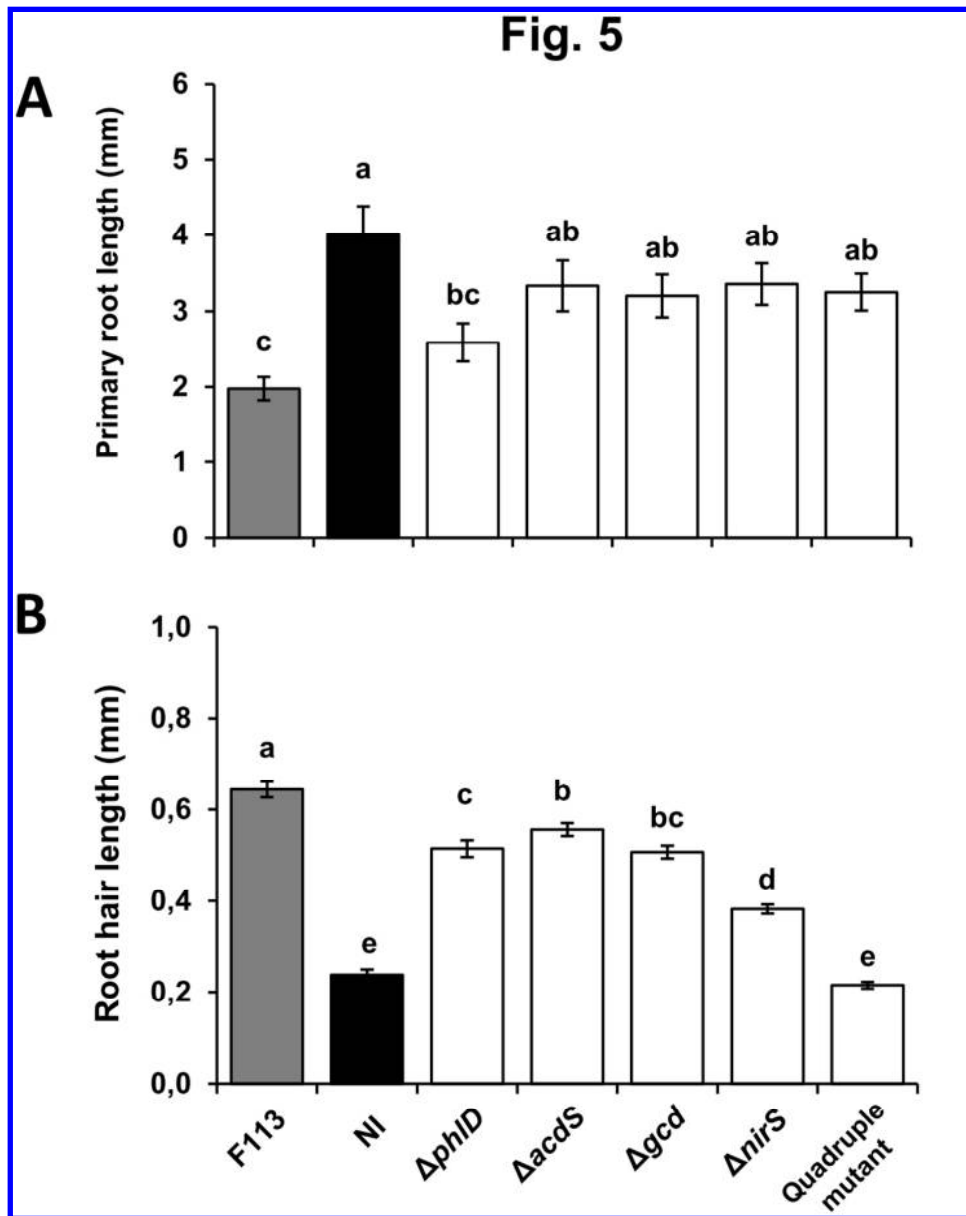


Fig. 5

113x142mm (300 x 300 DPI)

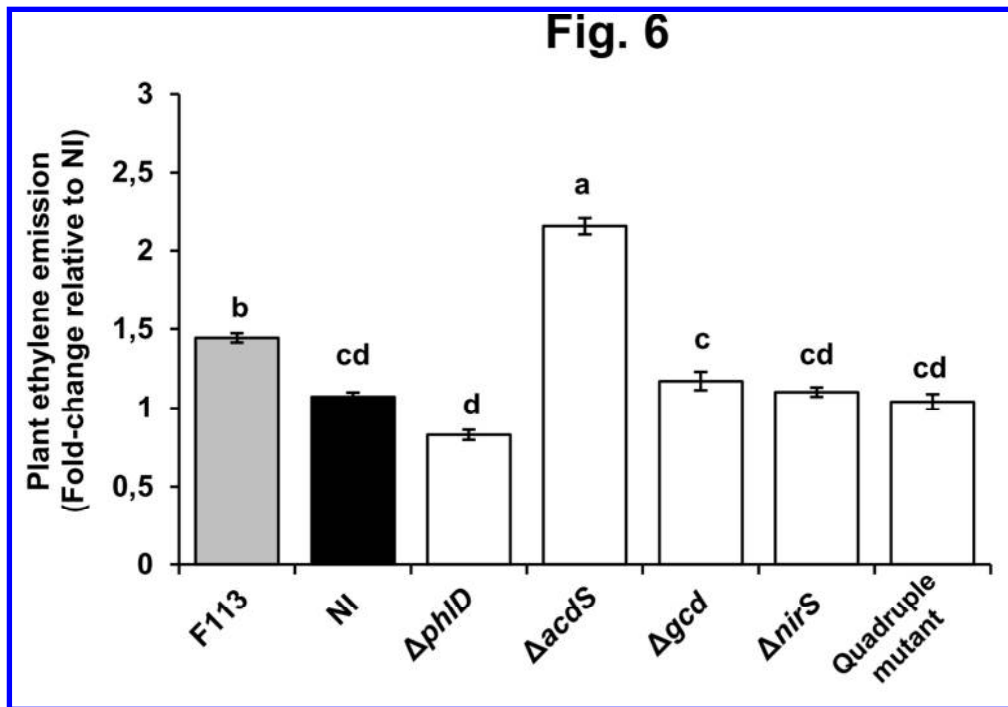


Fig. 6

118x81mm (300 x 300 DPI)

Comment citer ce document :

Vacheron, J., Desbrosses, G., Renoud, S., Padilla-Aguilar, R.-M., Walker, V., Muller, D., prigent-combaret, c. (Auteur de correspondance) (2018). Differential contribution of plant-beneficial functions from *Pseudomonas kilonensis* F113 to root system architecture alterations in *Arabidopsis thaliana* and *Zea mays*. *Molecular Plant-Microbe Interactions*. 31 (2). 212-223. . DOI :

Supplementary data

Vacheron *et al.*

Molecular Plant-Microbe Interactions

This paper has been peer reviewed and accepted for publication but has not yet been copyedited or proofread. The final published version may differ.

"First Look" paper • <http://dx.doi.org/10.1094/MPMI-07-17-0185-R> • posted 10/03/2017

Comment citer ce document :

Vacheron, J., Desbrosses, G., Renoud, S., Padilla-Aguilar, R.-M., Walker, V., Muller, D., prigent-combare, c. (Auteur de correspondance) (2018). Differential contribution of plant-beneficial functions from *Pseudomonas kilonensis* F113 to root system architecture alterations in *Arabidopsis thaliana* and *Zea mays*. *Molecular Plant-Microbe Interactions*. 31 (2). 212-223. . DOI :

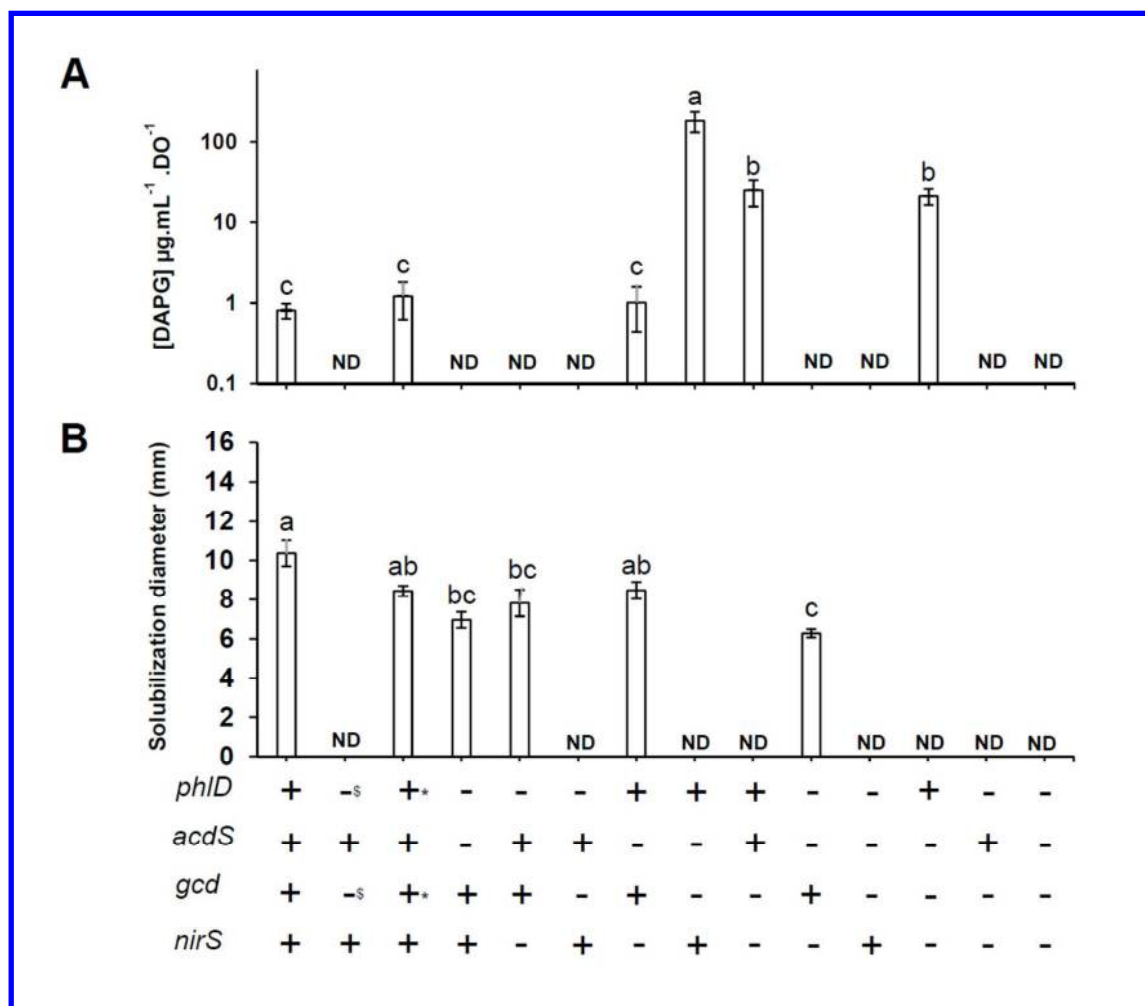


Fig. S1: Effect of the deletion (simple, double, triple, quadruple) of F113 plant beneficial functions (PBFs) on the production of 2,4-diacetylphloroglucinol (A) and phosphate solubilization activities (B). ND: non-detected. Statistical differences between strains for each tested PBF are indicated with letter a-c. Error bars correspond to standard error. (ANOVA and Tukey's HSD test, $P < 0.05$). ^s: results obtained for the 2 simple mutants $\Delta phlD$ or Δgcd (reminder from Fig. 1); * : results obtained for the complemented $\Delta phlD$ and Δgcd mutants.

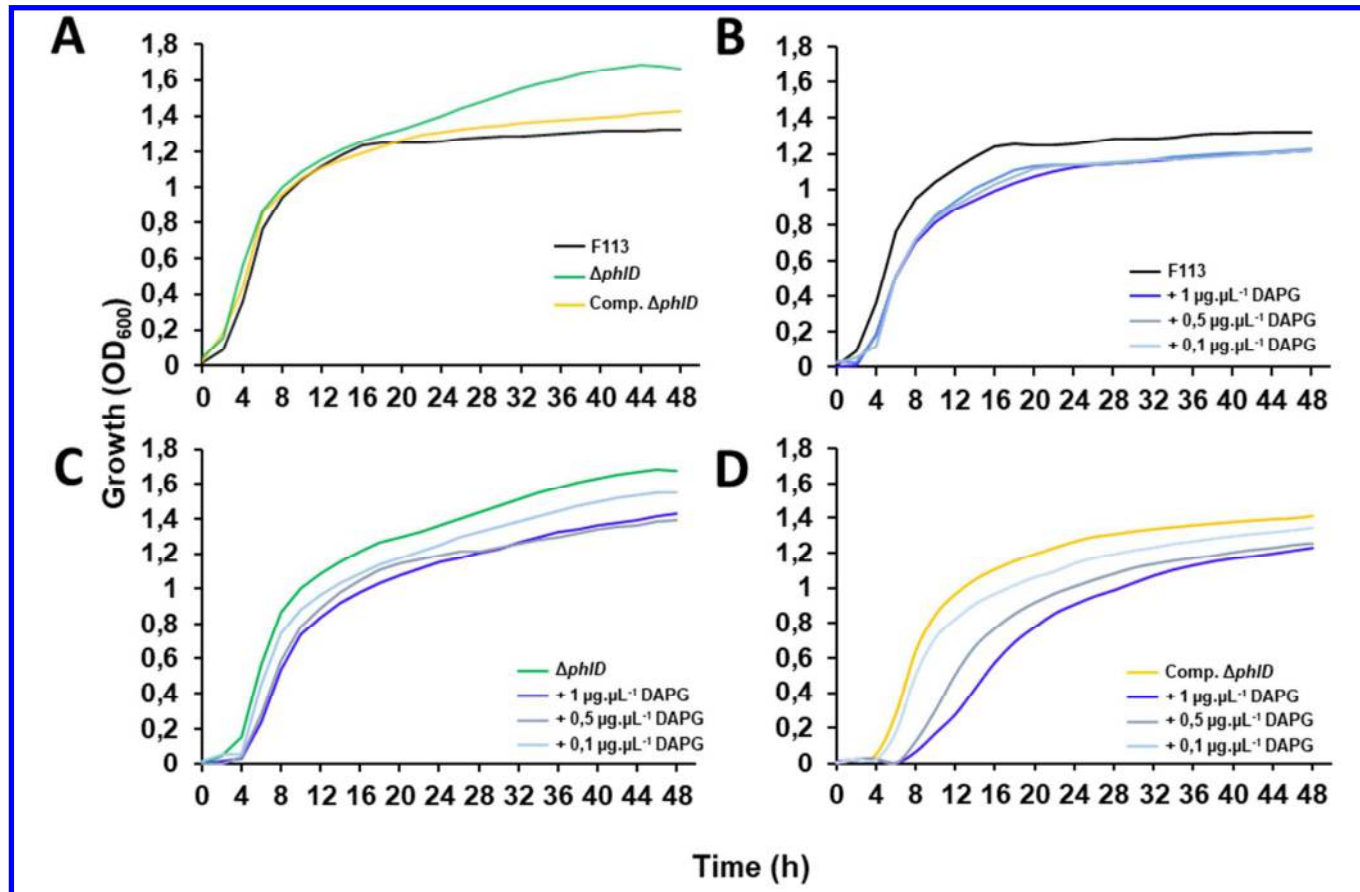


Fig. S2: Effect of the addition of DAPG on growth curves of the *P. fluorescens* wild-type F113, the $\Delta phlD$ mutant, and the $\Delta phlD$ complemented mutant with restored DAPG production.

Growth curves of F113 WT, $\Delta phlD$ and complemented $\Delta phlD$ (A). Effect of increasing DAPG concentrations on F113 WT (B), the $\Delta phlD$ mutant (C) and the complemented $\Delta phlD$ mutant (D). Comp.: Complemented. Results are presented as means of five replicate cultures (standard deviations were not presented but lower than 10%). The experiment was done three times independently.

Comment citer ce document :

Vacheron, J., Desbrosses, G., Renoud, S., Padilla-Aguilar, R.-M., Walker, V., Muller, D., prigent-combare, c. (Auteur de correspondance) (2018). Differential contribution of plant-beneficial functions from *Pseudomonas kilonensis* F113 to root system architecture alterations in *Arabidopsis thaliana* and *Zea mays*. *Molecular Plant-Microbe Interactions*. 31 (2). 212-223. . DOI :

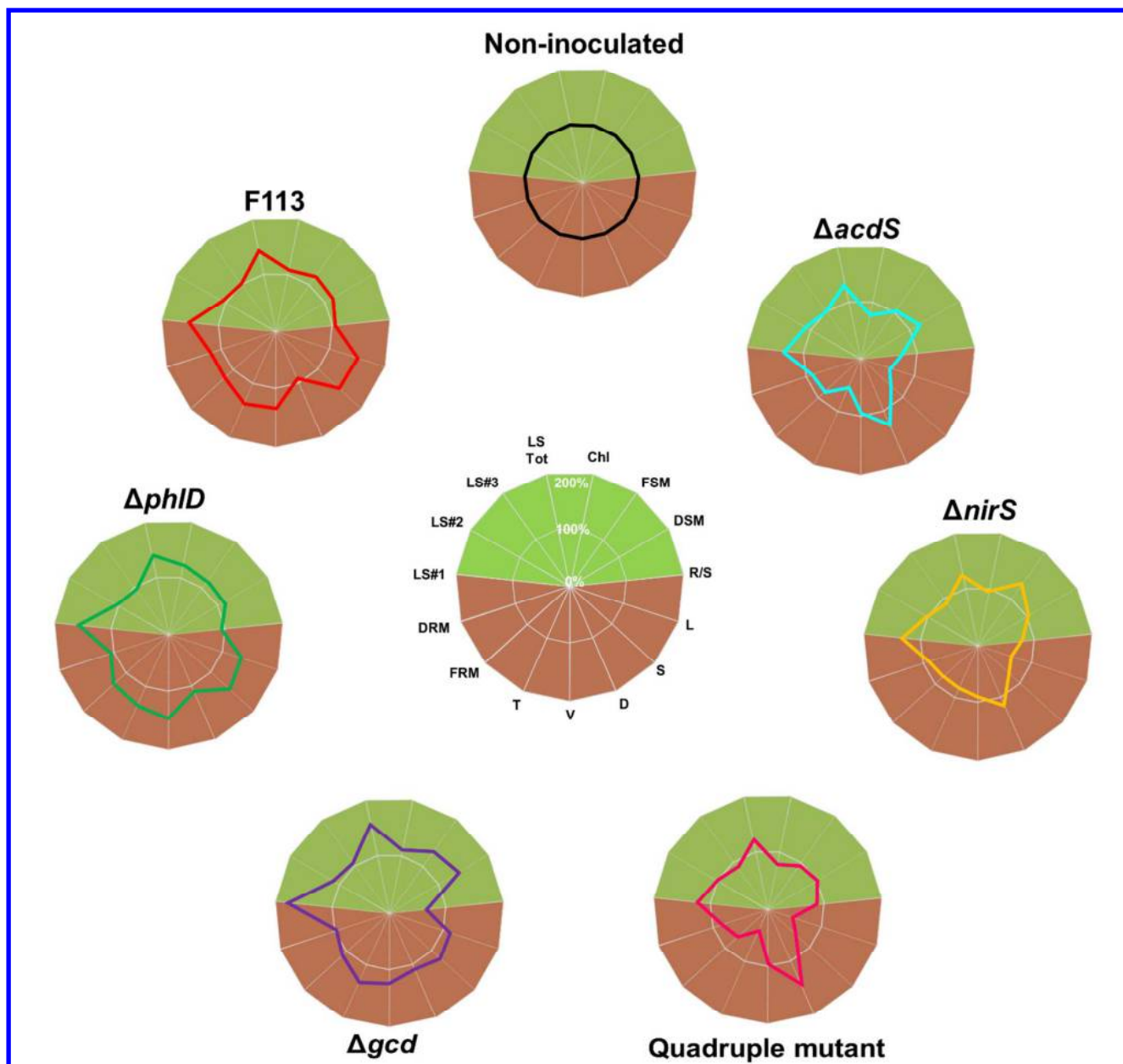


Fig. S3: Effects of *P. fluorescens* F113 and its PBF mutants on maize growth.

For each plant parameters, ratio between data obtained with mutants and with F113 were calculated and expressed in percent. Root and shoot measured parameters are colored respectively in brown and green on the star plot. **LS#1**: surface of the leaf number 1 (same nomenclature for leaf 2 and 3); **LSTot**: Total leaf surface; **Chl**: chlorophyll content in leaf number 3 measured with a chlorophyll content meter (Hansatech instruments model CL-01; Dinç et al. 2012); **FSM**: Fresh shoot mass; **DSM**: Dry shoot mass. **L**: total root length, **S**: Total root surface; **D**: Root diameter; **V**: root volume; **T**: Root tips; **FRM**: Fresh root mass; **DRM**: Dry root mass. **R/S** ratio represents the ratio between the dry root biomass and the dry shoot biomass.

Dinç, E., Ceppi, M.G., Tóth, S.Z., Bottka, S., Schansker, G. 2012. The chl a fluorescence intensity is remarkably insensitive to changes in the chlorophyll content of the leaf as long as the chl a/b ratio remains unaffected. *Biochim. Biophys. Acta* 1817:770-779.

Comment citer ce document :

Vacheron, J., Desbrosses, G., Renoud, S., Padilla-Aguilar, R.-M., Walker, V., Muller, D., prigent-combarete, c. (Auteur de correspondance) (2018). Differential contribution of plant-beneficial functions from *Pseudomonas kilonensis* F113 to root system architecture alterations in *Arabidopsis thaliana* and *Zea mays*. *Molecular Plant-Microbe Interactions*. 31 (2). 212-223. . DOI :

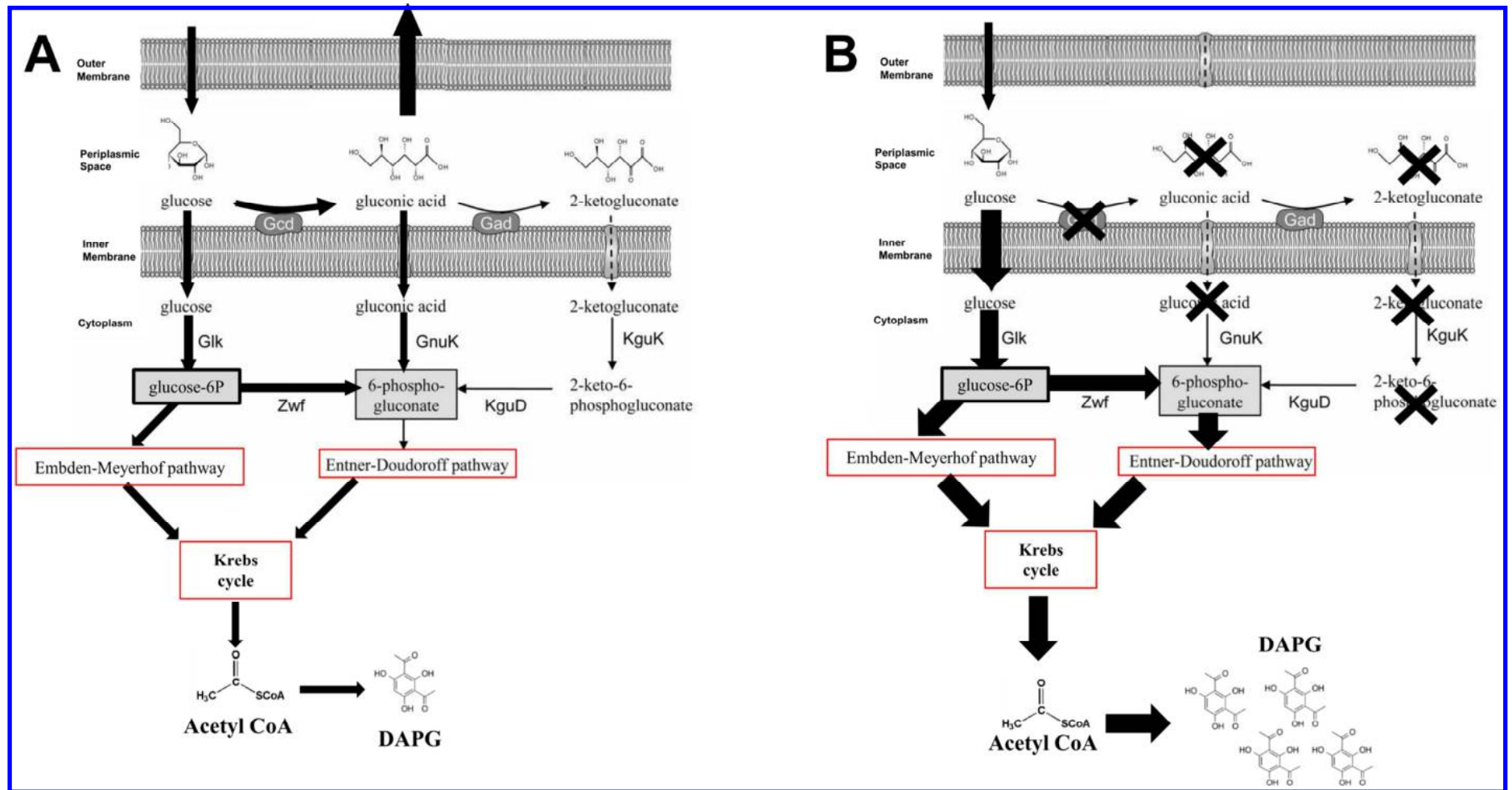


Fig. S4: Model presenting potential metabolic regulation involved in DAPG production in *P. fluorescens* F113.

Glucose catabolism in F113 (A) and F113 *gcd* mutant (B). Enzymes involved in glucose metabolism are abbreviated using the same nomenclature as de Werra *et al.* (2009). The corresponding enzyme functions and F113 gene names are indicated in parenthesis: Gcd (glucose dehydrogenase - *gcd*); Glk (glucokinase - *PSF113_1279*), Gad (Gluconate dehydrogenase - *PSF113_4842*); Zwf (glucose-6-phosphate-1-dehydrogenase - *PSF113_1290* and *PSF113_2674*); GnuK (gluconokinase - *PSF113_1311*); KguD (2-ketogluconate 6-phosphate reductase - *kguK*); KguK (2-ketogluconate kinase - *kguK*).

de Werra, P., Péchy-Tarr, M., Keel, C., Maurhofer, M. 2009. Role of gluconic acid production in the regulation of biocontrol traits of *Pseudomonas fluorescens* CHA0. *Appl. Environ. Microbiol.* 75:4162–4174.

Comment citer ce document :

Vacheron, J., Desbrosses, G., Renoud, S., Padilla-Aguilar, R.-M., Walker, V., Muller, D., prigent-combare, c. (Auteur de correspondance) (2018). Differential contribution of plant-beneficial functions from *Pseudomonas kilonensis* F113 to root system architecture alterations in *Arabidopsis thaliana* and *Zea mays*. *Molecular Plant-Microbe Interactions.* 31 (2). 212-223. . DOI :

Table S1: Slope comparison at the exponential growth stage and OD₆₀₀ at the stationary phase for F113 WT and its PBF mutants,

Strains	Growth curve slopes at exponential growth stage	OD ₆₀₀ at the stationary phase
F113 WT	0.20 ± 0.02 b	1.29 ± 0.06 b
<i>ΔphlD</i>	0.20 ± 0.02 b	1.54 ± 0.05 a
<i>ΔacdS</i>	0.17 ± 0.04 b	1.29 ± 0.09 b
<i>Δgcd</i>	0.18 ± 0.03 b	1.37 ± 0.08 b
<i>ΔnirS</i>	0.18 ± 0.03 b	1.35 ± 0.12 b
Quadruple mutant	0.25 ± 0.02 a	1.52 ± 0.01 a

Data were presented as mean ± standard deviation. Letters indicate statistical relations between strains for each tested PBF activities (ANOVA and Tukey's HSD test, $P < 0.05$)

Table S2: Effect of *P. fluorescens* F113 and its related mutants on maize root architecture

	Total root length (cm)			Total root surface (cm ²)			Root diameter (mm)			Root total volume (cm ³)			Number of root tips			Fresh root weight (g)			Dry root weight (g)									
F113	301.28	±	61.68	a	70.96	±	11.68	a	0.81	±	0.05	b	1.35	±	0.17	ab	2636.00	±	755.92	a	1.39	±	0.14	a	0.18	±	0.04	a
<i>ΔphlD</i>	262.55	±	43.59	a	68.59	±	7.40	a	0.92	±	0.09	ab	1.50	±	0.13	a	2535.75	±	551.14	a	1.44	±	0.12	a	0.15	±	0.01	ab
<i>ΔacdS</i>	108.83	±	18.92	bc	35.47	±	3.97	bc	1.12	±	0.09	ab	0.96	±	0.08	ab	995.29	±	235.46	b	0.95	±	0.09	b	0.13	±	0.03	ab
<i>Δgcd</i>	223.32	±	61.34	b	56.39	±	9.04	bc	0.93	±	0.10	ab	1.23	±	0.12	ab	2486.00	±	592.98	a	1.24	±	0.11	ab	0.14	±	0.02	ab
<i>ΔnirS</i>	123.30	±	27.81	bc	35.71	±	5.44	bc	1.02	±	0.08	ab	0.86	±	0.10	b	1455.38	±	400.02	b	0.86	±	0.13	b	0.12	±	0.03	b
<i>ΔΔΔΔ</i>	86.85	±	17.69	c	30.81	±	4.35	c	1.26	±	0.13	a	0.94	±	0.16	ab	760.13	±	163.47	b	0.80	±	0.06	b	0.12	±	0.02	b
NI	201.23	±	51.83	bc	48.66	±	8.85	bc	0.90	±	0.11	ab	1.01	±	0.14	ab	1918.63	±	506.78	a	1.14	±	0.12	ab	0.14	±	0.04	ab

* AU: Arbitrary Unit. Different letters correspond to significant differences for each plant parameter (ANOVA coupled with HSD's Tukey test $P=0.05$).

Comment citer ce document :

Vacheron, J., Desbrosses, G., Renoud, S., Padilla-Aguilar, R.-M., Walker, V., Muller, D., prigent-combare, c. (Auteur de correspondance) (2018). Differential contribution of plant-beneficial functions from *Pseudomonas kilonensis* F113 to root system architecture alterations in *Arabidopsis thaliana* and *Zea mays*. *Molecular Plant-Microbe Interactions*. 31 (2). 212-223. . DOI :

Table S3: Effect of *P. fluorescens* F113 and its related mutants on maize aerial parts

	Leaf surface 1 (cm ²)			Leaf surface 2 (cm ²)			Leaf surface 3 (cm ²)			Total Leaf surface (cm ²)			Chlorophyll content (AU*)		Fresh shoot weight (g)		Dry shoot weight (g)		R/S ratio													
F113	22.91	±	2.50	a	14.22	±	0.63	a	6.39	±	0.33	a	43.52	±	3.18	a	9.03	±	0.95	ab	1.31	±	0.15	ab	0.14	±	0.02	ab	1.30	±	0.17	ab
<i>ΔphlD</i>	23.33	±	1.41	a	13.97	±	0.33	a	6.15	±	0.14	a	43.45	±	1.68	a	10.15	±	0.78	a	1.26	±	0.08	ab	0.14	±	0.01	ab	1.11	±	0.08	ab
<i>ΔacdS</i>	20.33	±	2.04	ab	14.90	±	0.75	a	6.46	±	0.51	a	41.69	±	3.01	ab	6.74	±	0.39	b	1.22	±	0.13	ab	0.16	±	0.02	ab	0.92	±	0.17	ab
<i>Δgcd</i>	26.29	±	2.00	a	14.54	±	0.36	a	6.50	±	0.21	a	47.33	±	2.37	a	9.19	±	0.80	ab	1.47	±	0.12	ab	0.18	±	0.01	a	0.81	±	0.05	b
<i>ΔnirS</i>	18.91	±	1.56	ab	12.84	±	0.55	a	5.44	±	0.32	a	37.20	±	2.17	ab	7.69	±	0.49	ab	1.52	±	0.21	a	0.13	±	0.01	ab	0.96	±	0.09	ab
<i>ΔΔΔΔ</i>	18.16	±	2.14	ab	13.43	±	0.80	a	5.54	±	0.32	a	37.13	±	3.21	ab	6.49	±	0.51	b	1.05	±	0.11	ab	0.12	±	0.01	ab	1.06	±	0.08	ab
NI	14.76	±	1.56	b	13.12	±	0.85	a	6.12	±	0.33	a	30.31	±	2.39	b	8.27	±	0.67	ab	1.12	±	0.18	b	0.13	±	0.02	b	1.26	±	0.15	a

* AU: Arbitrary Unit. Different letters correspond to significant differences for each plant parameter (ANOVA coupled with HSD's Tukey test $P=0.05$).

Comment citer ce document :

Vacheron, J., Desbrosses, G., Renoud, S., Padilla-Aguilar, R.-M., Walker, V., Muller, D., prigent-combare, c. (Auteur de correspondance) (2018). Differential contribution of plant-beneficial functions from *Pseudomonas kilonensis* F113 to root system architecture alterations in *Arabidopsis thaliana* and *Zea mays*. *Molecular Plant-Microbe Interactions*. 31 (2). 212-223. . DOI :

Table S4: Bacterial strains and plasmids used in this study

Bacterial strain or plasmid	Relevant Characteristics ^a	Source or reference
Bacterial Strains		
<i>Pseudomonas fluorescens</i>		
F113	Wild-type, <i>Phl</i> ⁺ , <i>acdS</i> ⁺ , <i>gcd</i> ⁺ , <i>nirS</i> ⁺ HCN ⁺	Shanahan et al. 1992
$\Delta phlD$	F113 strain <i>phlD</i> gene deleted	This study
$\Delta acdS$	F113 strain <i>acdS</i> gene deleted	This study
Δgcd	F113 strain <i>gcd</i> gene deleted	This study
$\Delta nirS$	F113 strain <i>nirS</i> gene deleted	This study
$\Delta phlD \Delta acdS \Delta gcd \Delta nirS$	F113 quadruple mutant	This study
$\Delta phlD$ Comp	$\Delta phlD$ with restored DAPG production capacity	This study
<i>Escherichia coli</i>		
JM109	Host strain for the plasmids transformation	Promega
Plasmids		
pGEM-T easy vector	Cloning vector; Amp ^r ;	Promega
pBBR1-MCS5	Cloning vector used for complementation, Gm ^r	Kovach et al. 1995
pCM184	Cloning vector used for homologous recombination, Amp ^r , Km ^r , Tc ^r	Marx and Lidstrom 2002
pCM157	Containing Cre recombinase activity, Amp ^r , Tc ^r	Marx and Lidstrom 2002
pGEM-T easy: <i>phlD</i>	<i>phlD</i> cloned into pGEM-T easy, Amp ^r	This study
pGEM-T easy:UP <i>phlD</i>	Upstream sequence of <i>phlD</i> cloned into pGEM-T easy, Amp ^r	This study
pGEM-T easy:DW <i>phlD</i>	Downstream sequence of <i>phlD</i> cloned into pGEM-T easy, Amp ^r	This study
pGEM-T easy:UP <i>acdS</i>	Upstream sequence of <i>acdS</i> cloned into pGEM-T easy, Amp ^r	This study
pGEM-T easy:DW <i>acdS</i>	Downstream sequence of <i>acdS</i> cloned into pGEM-T easy, Amp ^r	This study
pGEM-T easy:UP <i>gcd</i>	Upstream sequence of <i>gcd</i> cloned into pGEM-T easy, Amp ^r	This study
pGEM-T easy:DW <i>gcd</i>	Downstream sequence of <i>gcd</i> cloned into pGEM-T easy, Amp ^r	This study
pGEM-T easy:UP <i>nirS</i>	Upstream sequence of <i>nirS</i> cloned into pGEM-T easy, Amp ^r	This study
pGEM-T easy:DW <i>nirS</i>	Downstream sequence of <i>nirS</i> cloned into pGEM-T easy, Amp ^r	This study
pCM184: <i>phlD</i>	Upstream and downstream sequence of <i>phlD</i> into pCM184, Amp ^r , Km ^r , Tc ^r	This study
pCM184: <i>acdS</i>	Upstream and downstream sequence of <i>acdS</i> into pCM184, Amp ^r , Km ^r , Tc ^r	This study
pCM184: <i>gcd</i>	Upstream and downstream sequence of <i>gcd</i> into pCM184, Amp ^r , Km ^r , Tc ^r	This study
pCM184: <i>nirS</i>	Upstream and downstream sequence of <i>nirS</i> into pCM184, Amp ^r , Km ^r , Tc ^r	This study
pBBR1-MCS5: <i>phlD</i>	<i>phlD</i> cloned into pBBR1-MCS5, Gm ^r	This study

^a: Amp^r Ampicillin resistant; Km^r Kanamycin resistant; Tc^r Tetracycline resistant, Gm^r, Gentamycin resistant

Kovach, M.E., Elzer, P.H., Hill, D.S. et al. 1995. Four new derivatives of the broad-host-range cloning vector pBBR1MCS, carrying different antibiotic-resistance cassettes. *Gene* 166: 175–176; Marx, C.J., Lidstrom, M.E. 2002. Broad-host-range *cre-lox* system for antibiotic marker recycling in gram-negative bacteria. *Biotechniques* 33:1062–1067; Shanahan, P., O'Sullivan, D.J., Simpson, P., Glennon, J.D., O'Gara, F. 1992. Isolation of 2,4-diacetylphloroglucinol from a fluorescent *Pseudomonad* and investigation of physiological parameters influencing its production. *Appl. Environ. Microbiol.* 58:353–358.

Comment citer ce document :

Vacheron, J., Desbrosses, G., Renoud, S., Padilla-Aguilar, R.-M., Walker, V., Muller, D., prigent-combare, c. (Auteur de correspondance) (2018). Differential contribution of plant-beneficial functions from *Pseudomonas kilonensis* F113 to root system architecture alterations in *Arabidopsis thaliana* and *Zea mays*. *Molecular Plant-Microbe Interactions*. 31 (2). 212-223. . DOI :

Table S5: Primers used in this study

Targeted regions	Names of primers	Sequences	Sizes of amplification	Reference
Insertion verification into pGEMTeasy	M13 F M13 R	GTTTCCCAGTCACGAC CAGGAAACAGCTATGAC	Variable according to the cloned gene	Promega
Insertion verification into pBBR1-MCS5	pBBR1MCS5_F1 pBBR1MCS5_R1	TGCAAGGCGATTAAGTTGGGTA TATGACCATGATTACGCCAAGC	Variable according to the cloned gene	Kovach et al. 1995
<i>phlD</i> gene amplification	phlDCompF1 phlDCompR1	ACTTTATTGGCTTCTCGCCG GGGTGTCGGTGTTTTATCGG	1104pb	This study This study
pCM184 insertion site 1	S1F S1R	ACGGAAATGTTGAATACTCATACTC CGTTTCCCGTTGAATATGGC	Variable according to the cloned gene	This study This study
pCM184 insertion site 2	S2F S2R	GCAGTCTTAGATAACTTCG GGCTGGATCCTCTAGTGAG	Variable according to the cloned gene	This study This study
Upstream region of <i>phlD</i>	phlDF1 phlDR1	TAGAGGTACCAGGCCACTAA †CAATTGTGACAGACCGATAAAACACCG	700pb	This study This study
Downstream region of <i>phlD</i>	phlDF2 phlDR2	CATGACAAGTCCTCGGCGAGA GGGATTTTGCACATTACTGA	753pb	This study This study
Upstream region of <i>acdS</i>	acdSF1 acdSR1	TAAGCGTAGAACTGCTTTTGG ‡CAGCTGTAGAACGACAGTCGGAAGAT	773pb	This study This study
Downstream region of <i>acdS</i>	acdSF2 acdSR2	ATTCAGTCGTGTCAGGTTTT CATGACTCTGCTCCTTGATAT	724pb	This study This study
Upstream region of <i>gcd</i>	gcdF1 gcdR1	TTTCATCGATTTCGACTACG †CAATTGTAAGCCCAAGCTGCGCTC	793pb	This study This study
Downstream region of <i>gcd</i>	gcdF2 gcdR2	CATAGTGTGTTTCTCCGTGAC CTTATCAATCCCCATGACTC	750pb	This study This study
Upstream region of <i>nirS</i>	nirSF1 nirSR1	‡CAGCTGCAGCAGGTGTTGCAGTTG †CAATTGAAGAACGTGATCAAGGACAAG	711pb	This study This study
Downstream region of <i>nirS</i>	nirSF2 nirSR2	TTTTTTGTGGCTGATCAGCAT CTTCATCCCCTTGAGCAG	702pb	This study This study
External primer	phlDExtf phlDExtr	ATTGAAGGAACAGTAGCCAG TGCAAAGGATATCGATGTGG	2378/1334pb *	This study This study
External primer	acdSExtf acdSExtr	ACAGCGTGAGCATTAGACAA ACTCTTCAAGTTACCCGCAG	2896/1885pb	This study This study
External primer	gcdExtf gcdExtr	CCATGAACCGTGAAGGTATT GTCAGTACCGTGAAGAAACT	4357/1949pb	This study This study
External primer	nirSExtf nirSExtr	AGGAGAGGAAAGAACGGAT TTCAGCCAAAGTGGACATC	3550/1972pb	This study This study

†: MunI (MfeI) restriction site ; ‡: PvuII restriction site ; *: size in F113 WT / size in the deleted mutant

Kovach, M.E., Elzer, P.H., Hill, D.S. et al. 1995. Four new derivatives of the broad-host-range cloning vector pBBR1MCS, carrying different antibiotic-resistance cassettes. *Gene* 166: 175–176.

Comment citer ce document :

Vacheron, J., Desbrosses, G., Renoud, S., Padilla-Aguilar, R.-M., Walker, V., Muller, D., prigent-combare, c. (Auteur de correspondance) (2018). Differential contribution of plant-beneficial functions from *Pseudomonas kilonensis* F113 to root system architecture alterations in *Arabidopsis thaliana* and *Zea mays*. *Molecular Plant-Microbe Interactions*. 31 (2). 212-223. . DOI :